communications biology

A Nature Portfolio journal

Article

https://doi.org/10.1038/s42003-025-08149-x

Ubiquitin-activating enzyme1 (TgUAE1) acts as a key regulator of *Toxoplasma gondii* lytic cycle and homeostasis

Qi-xin Zhou[1,3], Dai-qiang Lu[1,3], Si-yu Tian[1], Yao Lv[1], Ming-wei Chen[1], Xin Tian[1], Yan-tao Wu[1], Fang-jun Luo[2], Feng Tan[1] ✉ & Ya-ni Mou[1] ✉

Ubiquitylation, regulated by the ubiquitin-proteasome system (UPS), is crucial for cell division and cycle transitions in *Toxoplasma gondii*. However, the primary E1 ubiquitin-activating enzyme (UAE1) in this process has been unclear. This study identified and characterized TGGT1_290290 (TgUAE1) as the canonical E1 enzyme in *T. gondii*. Through a combination of bioinformatics, biochemical, pharmacological, and genetic approaches, TgUAE1 was shown to exhibit typical E1 activity, particularly in forming K48- and K63-linked polyubiquitin chains. TAK-243, a UAE1 inhibitor, can effectively inhibit the ubiquitin pathway in *T. gondii*, as thermal stabilization experiments identified TgUAE1 as its intracellular target. Disruption of TgUAE1 severely impaired parasite homeostasis and suppressed the lytic cycle, highlighting its critical role in *T. gondii* fitness. Mutation of C634 in TgUAE1 confirmed that its enzymatic activity is essential for function. Transcriptomics and quantitative ubiquitin proteomics revealed TgUAE1 as a key regulator of the ubiquitination process and the broader gene expression network in *T. gondii*. These findings not only underscore the indispensable role of TgUAE1 in the life cycle of *T. gondii* but also offer valuable data that could inform future studies on parasite biology and the development of novel therapeutic strategies.

The obligate intracellular parasitic protozoan *Toxoplasma gondii* is widely distributed worldwide, with an estimated one-third of the global population infected by this parasite[1]. In addition to humans, *T. gondii* can infect over 200 animal species and result in toxoplasmosis[2]. Classified as an opportunistic pathogen, *T. gondii* typically causes infections that rarely exhibit severe symptoms in immunocompetent individuals and most other hosts. However, the primary concern lies in congenital infections during pregnancy, which can lead to miscarriage, stillbirth, developmental abnormalities, and other serious fetal diseases[1]. Humans can acquire the infection by consuming meat containing *T. gondii* cysts, leading to significant economic losses and societal challenges[3]. Current clinical anti-*T. gondii* drugs exhibit limited efficacy on tissue cysts[4], harsh profile of side effects[5], and other deficiencies[6]. Therefore, it is imperative to elucidate the mechanisms regulating the *T. gondii* lytic cycle and identify novel therapeutic targets for effective control of toxoplasmosis.

T. gondii goes through different developmental stages during its complex life cycle, which involves several levels of regulation, including a diverse array of post-translational modifications (PTMs)[7]. Among these PTMs, protein ubiquitination plays a pivotal role in governing cellular behavior. The ubiquitination process involves the categorization and site-specific modification of substrate proteins through a cascade of three enzymes: ubiquitin-activating enzyme (E1), ubiquitin-conjugating enzyme (E2), and ubiquitin ligase (E3)[8]. In the presence of ATP, the E1 enzyme adenylates the C-terminal of ubiquitin (Ub) to form a mixed acid anhydride, activating Ub via cysteine residues in the E1 active site. Following activation, Ub is transferred from E1 to E2, and with the assistance of E3, Ub is transferred onto the substrate protein to complete the ubiquitination process[9]. Most ubiquitinated substrate proteins are directed toward the proteasome pathway for degradation, thereby maintaining cellular homeostasis[10]. Additionally, ubiquitination may alter protein activity or subcellular localization, regulating crucial cellular processes such as gene transcription, cell cycle progression, and signal transduction[11,12].

As the initiation step of ubiquitination, the E1 enzyme is critical in facilitating the ubiquitination process. As the primary E1 enzyme, UAE1 activates over 99% of ubiquitin in mammalian cells, highlighting its central role in the ubiquitination process[13]. The structure of the UAE1 protein

[1]Department of Parasitology, School of Basic Medical Sciences, Wenzhou Medical University, Wenzhou, 325035 Zhejiang, China. [2]Department of Clinical Laboratory, Zhuji People's Hospital, Zhuji, Zhejiang, China. [3]These authors contributed equally: Qi-xin Zhou, Dai-qiang Lu. ✉e-mail: tanfengsong@163.com; mouyaniq@163.com

comprises six functional domains involved in Ub activation and transfer: the first catalytic cysteine domain (FCCH), inactive adenylation domain (IAD), active adenylation domain (AAD), second catalytic cysteine domain (SCCH), four-helix bundle (4HB), and ubiquitin fold domain (UFD). Among these domains, the SCCH domain contains catalytic cysteine residues crucial for Ub activation by forming a thioester bond with the C-terminal of Ub, subsequently transferring the activated Ub to the E2 enzyme[14].

Currently, the E1 family protein TGME49_314890[15], localized in the apicoplast (a unique organelle), and the ubiquitin-activated enzyme-like protein TGGT1_212100[16], involved in regulating protein import into the apicoplast, have been identified in *T. gondii*. However, the canonical E1 family protein responsible for ubiquitination in *T. gondii* remains unreported. Recently, the identification of E1 (PfUAE1, PF3D7_1225800) in *Plasmodium falciparum* (*P. falciparum*), another significant apicomplexan parasite, has shed light on its role in ubiquitin activation within the parasite[17]. Notably, researchers effectively inhibited PfUAE1 activity using TAK-243 (also known as MLN7243), a potent and specific UAE1 inhibitor, resulting in a phenotype consistent with the impeded schizont to merozoite conversion observed after PfUAE1 knockdown[17]. The UAE1 homolog of *T. gondii* exhibits distinct characteristics compared to the apicoplast E1 family protein. The present study demonstrated that the *T. gondii* homolog TgUAE1 functions as a canonical E1 protein with both in vivo and in vitro enzyme activity. Moreover, it plays a vital role in the lytic cycle and maintaining homeostasis, closely associated with activating integrated stress response signaling pathways. These results greatly extend our knowledge of parasite protein ubiquitylation and underscore the fundamental role of TgUAE1 in parasite biology, paving the way for further exploration into the molecular mechanisms governing apicomplexan parasite survival and pathogenesis.

Results

Identification and sequence characterization of TgUAE1 homolog from *T. gondii*

The TgUAE1 (ToxoDB: TGGT1_290290) sequence (NCBI accession EPR59782), annotated as an E1 family protein in the *T. gondii* genome, comprises 1092 amino acids (119.82 kDa). To elucidate the evolutionary relationship between TgUAE1 and E1 family genes across different species, various members of the E1 family[18] (Uba1, Uba2, Uba3, Uba4, and Uba5) as well as an E1-like enzyme, Atg7, were selected for analysis as an outgroup. We also included the Toxoplasma Atg7 homologue in our analysis to further enhance species-specific comparisons. Phylogenetic analysis revealed that TGGT1_290290 is most closely related to Uba1 (also known as UAE1); hence it is designated as TgUAE1 to distinguish it from the ubiquitin-like activating enzyme TgUba1[16] (TGGT1_212100, classified as Uba4 based on the phylogenetic tree) (Fig. 1A). Despite the relatively low overall sequence homology (Fig. S1A, identity = **55.19%**), TgUAE1 possesses conserved ubiquitin adenylation and cysteine catalytic sites (Cys634), as well as functional domains associated with E1 enzymes, including IAD, AAD, FCCH and SCCH (Fig. 1B, Fig. S1A). Structural conservation of these domains was further supported by homology modeling comparisons between TgUAE1 and ScUba1 (Fig. 1C, D), indicating TgUAE1's potential to activate ubiquitin.

TgUAE1 exhibits ubiquitin-activating enzyme activity in vivo and in vitro

To characterize the E1 enzyme activity of TgUAE1, the recombinant TgUAE1 fusion protein with an N-terminal glutathione transferase (GST) affinity tag was expressed and purified in *E. coli* (Fig. S2A and S2B). The purified GST-TgUAE1 protein was validated through western blotting (WB) analysis, revealing specific bands around 140 kDa (Fig. 2A). In vitro biochemical assays were then conducted to evaluate TgUAE1's ability to undergo Ub-E1 thioesterification and transfer of Ub to E2. The reaction condition included purified GST-TgUAE1, Flag-HsUb (human ubiquitin tagged with a Flag at the N-terminus), and ATP. In the presence of ATP, a distinct band at approximately 140 kDa, corresponding to the TgUAE1-Ub interaction, was detected (Fig. 2B, third lane from the left). The addition of the reducing agent DTT led to the disappearance of this band (Fig. 2B, fourth lane from the left), indicating that TgUAE1 interacts with Ub via thioesterification.

Next, HsCdc34 (human E2) was added to the reaction to investigate TgUAE1's ability to transfer Ub to E2. As expected, alongside the TgUAE1-Ub band, a distinct band at approximately 40 kDa, corresponding to Ub-E2, was observed (Fig. 2B, fifth lane from the left). The presence of DTT abolished both TgUAE1-Ub and Ub-E2 interactions (Fig. 2B, sixth lane from the left). In contrast, only inactive forms of Ub were detected in the absence of TgUAE1 (Fig. 2B, first and second lanes from the right).

The inhibitory potency of MLN7243 (TAK-243) against mammalian UAE1 has been demonstrated through the formation of conjugates with activated Ub, referred to as "TAK-243-Ub," and TAK-243 shows weaker inhibitory activity against other closely related E1 ubiquitin-like activating enzymes[19]. The docking of TAK-243 with TgUAE1 suggests a potential interaction that could impact the stability and function of TgUAE1, particularly influencing the enzyme's active site and potentially altering its thermal stability or activity in the presence of the compound (Fig. S1B). To investigate the importance of ubiquitylation, TAK-243 was introduced into the system to assess its potential inhibitory effect on TgUAE1-Ub thioesterification in vitro. A negative correlation was observed between the concentration of TAK-243 and the binding affinity of Ub to TgUAE1, concomitant with an increase in unbound Ub, identifying TAK-243 as particularly effective (Fig. 2C). Based on the in vitro results, the in vivo efficacy of TAK-243 in inhibiting *T. gondii* ubiquitination was further investigated through a WB analysis using an α-ubiquitin antibody (Fig. 2D). The effect of TAK-243 on the ubiquitination of TgUAE1 was assessed in both parasite and host cell. In the presence of TAK-243 (3 μM and 5 μM), a noticeable decrease in the Ub-TgUAE1 bands is observed, suggests that TAK-243 inhibits the enzymatic activity of TgUAE1, leading to lower levels of parasite ubiquitination. Although TAK-243 also exerts a similar effect on host cell ubiquitination, the host cell protein content in the parasite lysates is minimal, which has a negligible impact on the overall result. Therefore, the observed decrease in TgUAE1 ubiquitination is primarily attributed to the direct action of TAK-243 on the parasite's ubiquitin-activating enzyme activity.

To determine whether TgUAE1 is a potential target of TAK-243, a single-crossover homologous recombination strategy was employed to insert a triple-HA (3HA) epitope tag at the C-terminus of endogenous TgUAE1 protein (Fig. S2C). The successful construction of the TgUAE-3HA transgenic strain was confirmed through WB analysis (Fig. S2D) and immunofluorescence assay (IFA) (Fig. S2E), utilizing an α-HA antibody. To assess any potential impact of C-terminal tagging on parasite proliferation capacity, a plaque assay was conducted, revealing that the proliferation ability of the TgUAE1-3HA strain was comparable to that of the parental strain ($p > 0.05$) (Fig. S2F and S2G).

Proteins from both the parental and transgenic strain were extracted, and immunoprecipitation was performed using magnetic beads coated with anti-HA antibodies. The precipitated samples were subjected to mass spectrometry analysis, successfully detecting TgUAE1(Fig. S2H), further confirming the successful construction of the transgenic strain TgUAE1-3HA. Additionally, specific peptides of TgUb were detected in these samples (Fig. S2I), indicating an interaction between TgUAE1 and TgUb, suggesting that TgUAE1 may serve as a ubiquitin-activating enzyme.

A thermal stability experiment, a common approach for investigating drug-target interactions[20] and successfully used in *Leishmania*, *Plasmodium* and *Toxoplasma*[21,22], was performed to evaluate the stability of TgUAE1 in the presence of TAK-243 under high-temperature conditions. In the presence of TAK-243, TgUAE1 shows significantly higher stability compared to the absence of TAK-243 at temperatures between 43 °C and 56 °C (Fig. 2E, F). A comparison of the treatments with and without TAK-243 on the same gel revealed that as the temperature increased, the intensity of the TgUAE1 band progressively decreased in the absence of TAK-243,

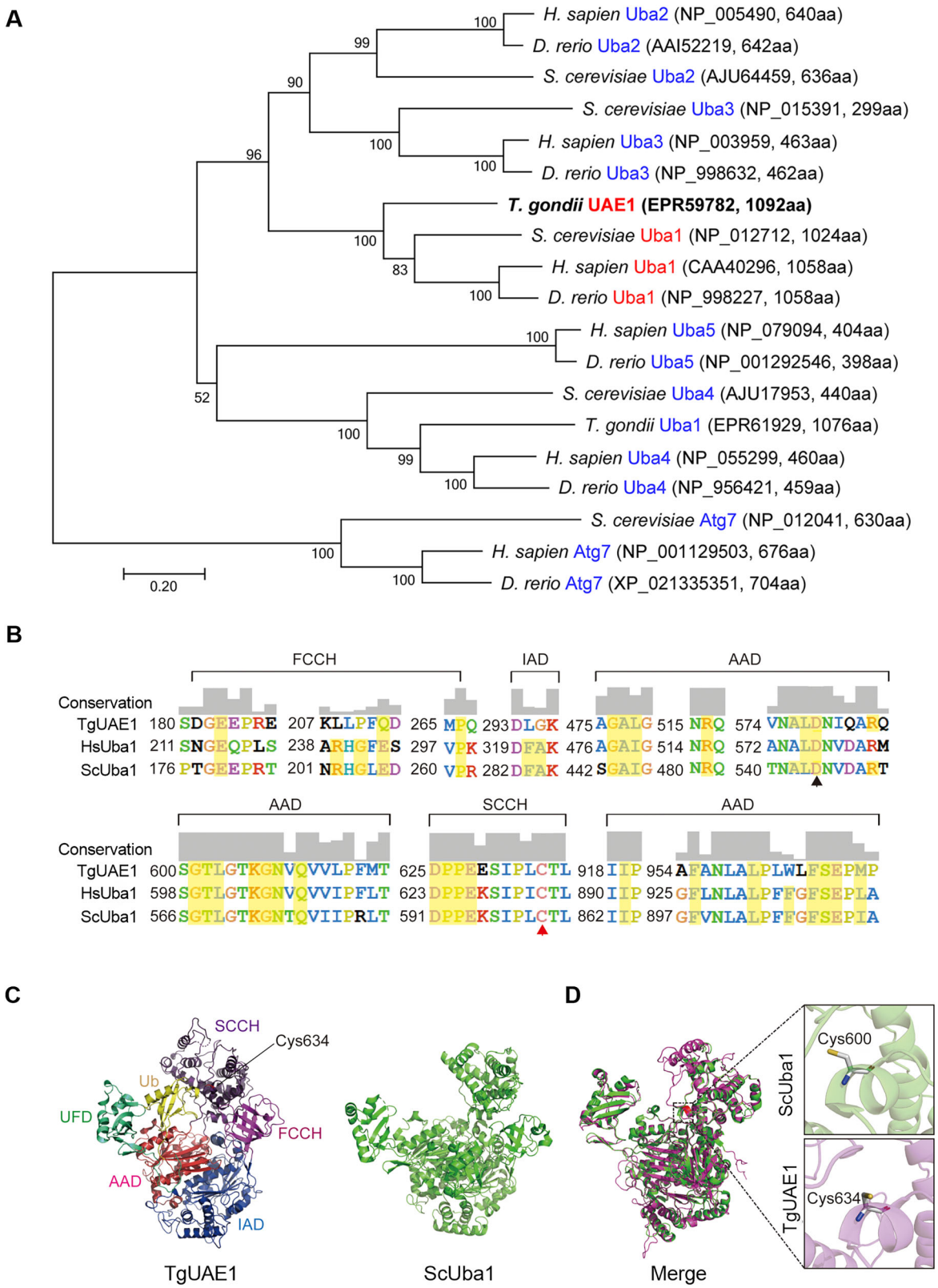

Fig. 1 | Protein sequence alignment and structural analysis of TgUAE1. A The phylogenetic relationships of TgUAE1 homologs found in *Homo sapiens*, *Saccharomyces cerevisiae*, and *Danio rerio*. The *T. gondii*_TgUAE1 was bolded in the present study. The branch lengths are proportional to genetic distances, assessed using the neighbor-joining method in MEGA7 (http://www.megasoftware.net/). **B** The amino acid sequence of *T. gondii* UAE1 (TgUAE1) is compared to that of *H. sapiens* UAE1 (HsUba1) and *S. cerevisiae* UAE1 (ScUba1). The conserved cysteine catalytic site is marked by a red arrow, while the ubiquitin adenylation site is marked by a black arrow. The functional domain associated with the ubiquitin-activating enzyme E1 is indicated as FCCH.IAD.AAD.SCCH. **C** The structural conformation of the TgUAE1 protein was predicted using RaptorX software, which also generated a comprehensive binding diagram illustrating potential interactions with ubiquitin (Ub). Additionally, the presence of a ubiquitin fold domain (UFD) was identified. **D** PyMOL software was utilized to superimpose the structures of TgUAE1 and ScUba1 proteins for comparative analysis. Cys600 represents the cysteine catalytic site in ScUba1, whereas Cys634 corresponds to the cysteine catalytic site in TgUAE1.

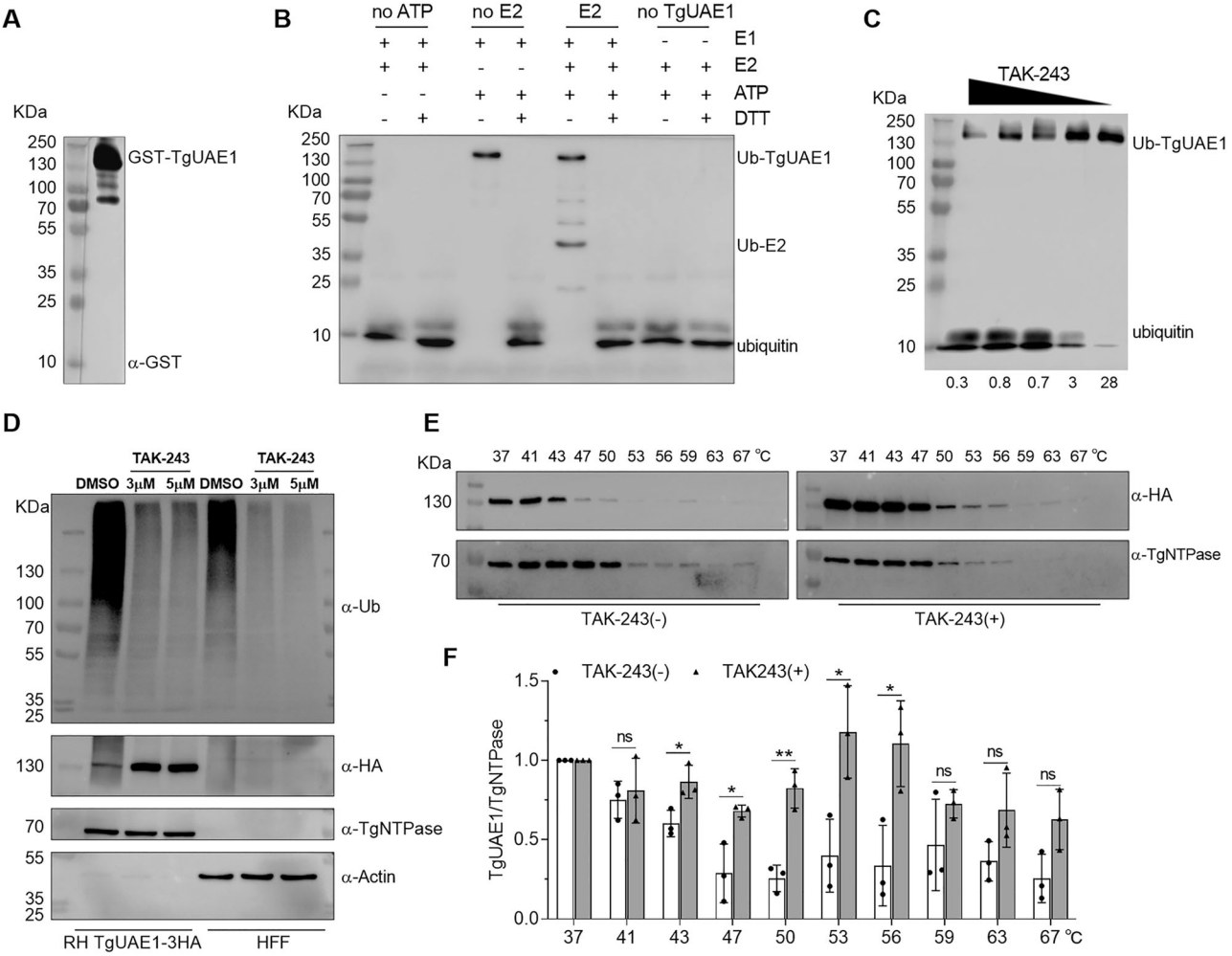

Fig. 2 | Validation of ubiquitin-activating enzyme activity of TgUAE1 in vitro and in vivo. A The purified GST-TgUAE1 protein was verified by WB using an anti-GST antibody. **B** The thioesterification activity of TgUAE1 was assessed using FLAG-labeled ubiquitin (Ub) and the transthioesterification to E2 (CDC34) in vitro. Thioesterification of E1 by Ub occurs in the absence of E2; in the presence of E2 (CDC34), further transthioesterification to E2 is observed. No thioester formation occurs without ATP or after treatment with DTT. **C** The covalent addition of ubiquitin to TgUAE1 in vitro is reduced with increasing concentrations of TAK-243. The concentrations of TAK-243 used were 0.3125 μM, 0.625 μM, 1.25 μM, 2.5 μM, and 5 μM (from left to right), the corresponding grayscale values for the Ub-TgUAE1 bands are shown beneath each lane. **D** The level of tachyzoite ubiquitylation in vivo was assessed in both TgUAE1-3HA strain and HFF cells treated with DMSO or TAK-243 (3 μM and 5 μM). WB was performed using anti-ubiquitin (α-Ub) antibody to detect global ubiquitylation. Anti-HA (α-HA) was used to detect TgUAE1-3HA, while α-TgNTPase and α-Actin were used as loading controls. **E** Thermal stability assays indicate that TgUAE1 stability is temperature-sensitive. In the absence of TAK-243, TgUAE1 protein stability decreases progressively with increasing temperatures (37 °C to 67 °C). In the presence of TAK-243, TgUAE1 stability is maintained at temperatures between 37 °C and 56 °C, but decreases at higher temperatures. TgNTPase was used as a loading control. **F** Quantification of the thermal stability of TgUAE1 using grayscale analysis. The ratio of TgUAE1 to TgNTPase intensity was plotted for each temperature condition. In the presence of TAK-243, TgUAE1 shows significantly higher stability compared to the absence of TAK-243 at temperatures between 43 °C and 56 °C (*$p < 0.05$, **$p < 0.01$). Statistical significance was determined using a *t*-test. Data represent mean ± SD from three independent experiments.

especially at temperatures above 50 °C. In contrast, under TAK-243 treatment, the stability of TgUAE1 was notably enhanced (Fig. S1C).

These findings demonstrate that TgUAE1 can activate Ub and transfer it to E2, confirming its status as a canonical E1 family protein. Additionally, the results indicate that TgUAE1 is a promising target of TAK-243, and its enzymatic activity may be susceptible to inhibition by TAK-243.

TAK-243 inhibits *T. gondii* proliferation

Given the inhibitory efficiency of TAK-243 on the enzymatic activity of TgUAE1, its impact on the proliferation of *T. gondii* was investigated by IFA. Compared to the DMSO control group, TAK-243 treatment significantly inhibited intracellular tachyzoite proliferation, as evidenced by the predominance of PVs containing 2 or 4 parasites, with some fields showing up to 8 or 16 parasites (Fig. 3A, B). Subsequently, a luminescence-based β-galactosidase (β-Gal) activity assay[23] was employed to determine the 50% effective concentration (EC_{50}) of TAK-243 against parasite proliferation using the RH-2F strain[24]. The results demonstrated a potent inhibitory effect of TAK-243 on parasite proliferation, with an EC_{50} value of 118.7 nM (Fig. 3C). To assess the potential impact of TAK-243 on host cell viability, we determined the half-maximal lethal concentration (CC_{50}) of TAK-243 for HFFs. The CC_{50} for HFFs was calculated to be 136.2 nM (Fig. 3D). The therapeutic index (TI), defined as the ratio of CC_{50} to EC_{50}, was 1.15, indicating that the difference between the drug's toxicity to host cells and its efficacy against *T. gondii* is relatively small. This suggests that while TAK-243 is effective in inhibiting parasite proliferation, it may also have potential toxicity to host cells. Therefore, caution should be taken in adjusting the dosage or considering combination therapies to minimize host cell toxicity. Additionally, the impact of TAK-243 on subcellular organelles in the TgUAE1-3HA strain was examined using IFA. The results indicated that TgUAE1 exhibited a diffuse cytoplasmic distribution (green) during the

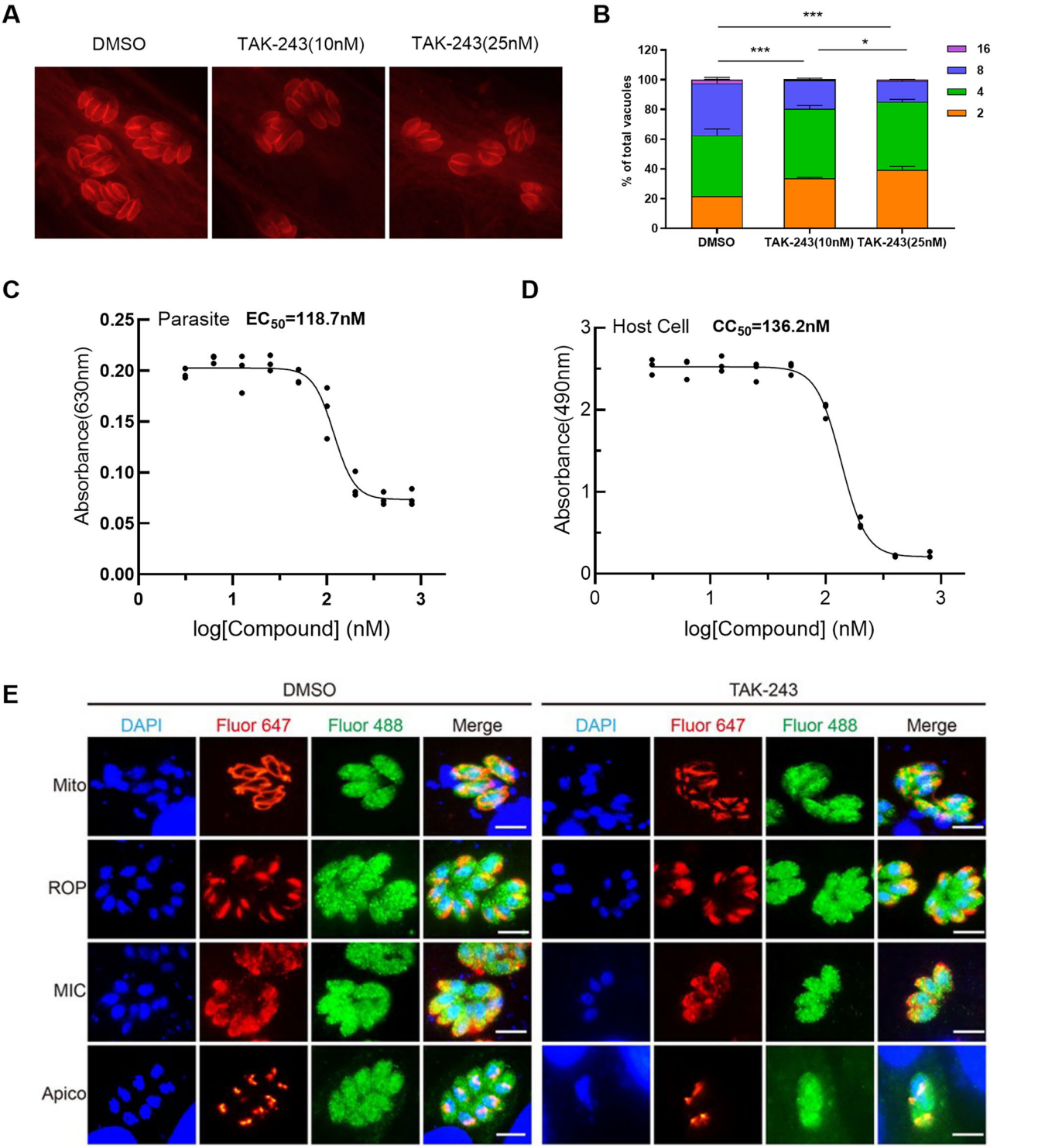

Fig. 3 | Impact of the UAE1-specific inhibitor TAK-243 on *T.gondii*. **A** The presence of tachyzoites in host cells following a 24 h treatment with DMSO or TAK-243 (10 nM or 25 nM) was observed by IFA using an anti-TgSAG1 antibody. **B** The proportion of vacuoles containing different numbers of parasites relative to the total number of vacuoles was assessed following treatment with DMSO or TAK-243 (10 nM or 25 nM) for 24 h. Data are presented as means ± SD, and statistical significance was determined using a one-way ANOVA (*$p < 0.05$, ***$p < 0.001$). **C** The EC_{50} represents the concentration of TAK-243 required to achieve 50% inhibition of *T. gondii* proliferation. **D** Cytotoxicity of TAK-243 on HFFs, shown as a dose-response curve with a CC_{50} value of 136.2 nM, measured by absorbance. **E** The impact of TAK-243 on the morphology of subcellular organelles in *T. gondii* was observed by IFA using specific antibodies against F1 beta ATPase (mitochondria), ROP1 (rhoptry), MIC3 (microneme), and Cpn60 (apicoplast). Alexa Fluor 647-labeled secondary antibodies indicated subcellular organelles in red fluorescence. Additionally, the localization of TgUAE1-3HA transgenic parasites was visualized using an anti-HA antibody and Alexa Fluor 488-labeled secondary antibody in green fluorescence (scale: 5 μm).

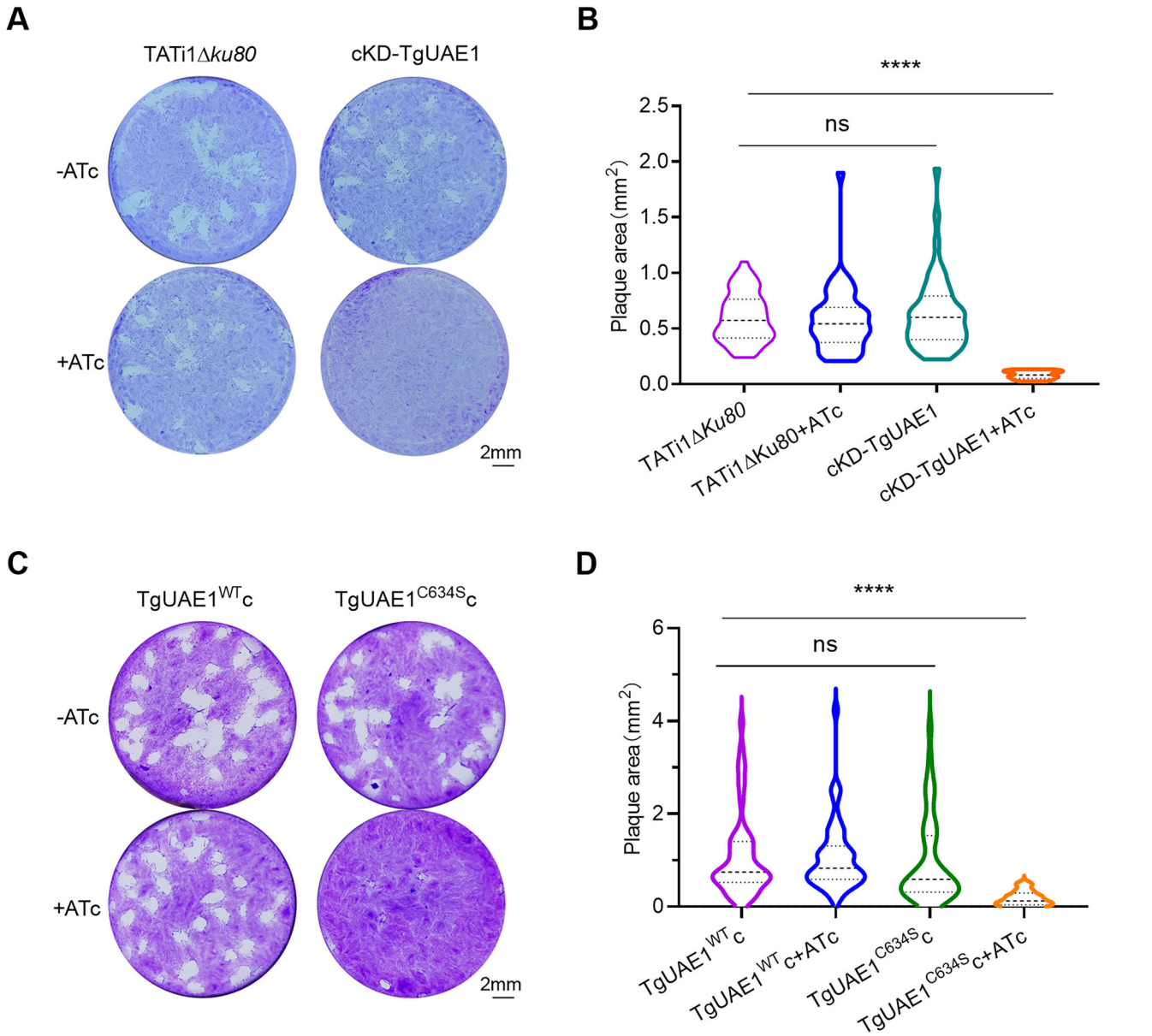

Fig. 4 | Effect of TgUAE1 on the growth of *T. gondii*. **A** The plaque assay was performed by inoculating HFFs infected with the cKD-TgUAE1, compared to TATi1 Δ*Ku80*, with or without ATc treatment for 7 d. Scale bar = 2 mm. **B** The statistical results of the plaque assay are presented as violin plots showing the distribution of plaque areas from three biological replicates. Statistical significance was analyzed using the Kruskal-Wallis test (ns $p > 0.05$, **** $p < 0.0001$). **C** The plaque assay was conducted by inoculating HFFs infected with the TgUAE1^{C634S}c mutant strain, compared to the TgUAE1^{WT}c strain, with or without ATc treatment for 7 d. Scale bar = 2 mm. **D** The statistical results of the plaque assay are presented as violin plots showing the distribution of plaque areas from three biological replicates. Statistical significance was analyzed using the Kruskal-Wallis test (ns $p > 0.05$, ****$p < 0.0001$).

intracellular proliferation phase, displaying varying degrees of colocalization with mitochondria, rhoptry, microneme, and apicoplast. Notably, TAK-243 treatment significantly disrupted mitochondrial morphology, suggesting that TgUAE1 may play a role in maintaining mitochondrial structural integrity (Fig. 3E).

TgUAE1 and its catalytic activity are indispensable for tachyzoites growth

Based on the above findings, we attempted to establish a stable TgUAE1 knockout strain. However, multiple unsuccessful attempts indicated that TgUAE1 is essential for the growth and development of *T. gondii*, consistent with its significantly low CRISPR phenotype score of −4.25[25]. Consequently, a TgUAE1 knockdown strain (cKD-TgUAE1) with an N-terminal 3HA epitope tag was generated by replacing the native promoter of TgUAE1 with an anhydrotetracycline (ATc)-regulated promoter (Fig. S3A). PCR confirmed the successful replacement of the endogenous promoter in two stable monoclonal strains (Fig. S3B, primers listed in Supplementary Data 1). WB and RT-qPCR demonstrated that 4-day ATc treatment significantly reduced TgUAE1 protein and transcript levels in both monoclonal strains (Fig. S3C and S3D).

To evaluate the impact of TgUAE1 knockdown on the overall lytic ability of *T. gondii* over an extended period, plaque assays were conducted (Fig. 4A). Compared to the parental and non-ATc-treated cKD-TgUAE1 strains, ATc-treated cKD-TgUAE1 parasites exhibited a severe defect in plaque formation (Fig. 4B). To validate the correlation between the plaque defect and TgUAE1 depletion, as well as to assess the function of the cysteine catalytic site in TgUAE1 (Cys634), complementary strains expressing the full-length UAE1 protein: TgUAE1^{WT}c (Fig. S3F) and mutant strains with a Cys634 mutation: TgUAE1^{C634S}c (Fig. S3G and S3H) were generated based on the parental strain cKD-TgUAE1. Repeating the plaque assays, it was

observed that complementation with constitutively expressed 3FLAG-TgUAE1^{WT} restored plaque formation in cKD-TgUAE1 parasites cultured in the presence of ATc (Fig. 4C, D). This finding suggests that the growth defect was specifically due to the loss of TgUAE1, and that the complementary strain TgUAE1^{WT}c can be used as a control for the mutant strain TgUAE1^{C634S}c in subsequent experiments. Conversely, complementation with constitutively expressed TgUAE1^{C634S}c (Fig. 4C) did not rescue the plaque formation defect. Although small plaques were observed in the catalytic dead mutant, this could be attributed to residual enzymatic activity or compensatory mechanisms within the parasites, which may partially sustain tachyzoite growth. Despite this, the catalytic dead mutant consistently exhibited significantly smaller plaque areas compared to the complementary strain TgUAE1^{WT}c under identical conditions (Fig. 4D). This observation underscores the essential role of TgUAE1's catalytic activity in tachyzoite proliferation and plaque formation, indicating that the enzymatic function is critical for optimal parasite growth and replication.

A comprehensive evaluation of each stage in the lytic cycle of *T. gondii* was conducted following TgUAE1 depletion or mutation at the TgUAE1-Cys634 site, specifically focusing on gliding (Fig. 5A, B), invasion (Fig. 5C), intracellular proliferation (Fig. 5D), and egress (Fig. 5E). TgUAE1 knockdown inhibited the gliding ability, invasion, intracellular proliferation, and egress of tachyzoites. In contrast, the TgUAE1-Cys634S mutation impaired tachyzoite proliferation and gliding ability, but did not affect invasion or egress abilities in the presence of ATc. These findings indicate that TgUAE1 regulates different aspects of *T. gondii* biology through distinct mechanisms, where its role in motility is primarily dependent on its ubiquitin-activating enzyme activity, but its regulation of invasion and egress might involve other factors. While we cannot entirely exclude the possibility that TgUAE1 knockdown or mutation of its active site may affect overall parasite viability, our data clearly demonstrate the essential role of TgUAE1 in regulating the lytic cycle of *T. gondii*, with its Cys634 site playing a particularly critical role.

The effect of TgUAE1 on the subcellular organelle of *T. gondii*

Given our previous observations of mitochondrial fragmentation induced by TAK-243 treatment (Fig. 3D) and the close spatial proximity between mitochondria and the apicoplast, IFA was conducted to examine the morphological and quantitative alterations in both TgUAE1 depletion and TgUAE1-C634S mutation strains. The results demonstrated that while depletion of TgUAE1 or mutation of Cys634 did not significantly affect apicoplast homeostasis (Fig. 6A, B), there was a severe defect in mitochondrial morphology. For instance, the cKD-TgUAE1 strain exhibited mitochondrial fragmentation after 48 h of ATc treatment, with more pronounced changes observed after 72 h. By 96 h, nearly all mitochondria displayed deformation, transitioning from their normal ring or sperm shapes to abnormal spots or fragments following complete TgUAE1 knockdown. These impairments were also observed in the TgUAE1^{C634S}c strain treated with ATc for 96 h. In contrast, mitochondrial morphology remained normal in TATi1 Δ*ku80* parasites after 96 h of ATc treatment (Fig. 6C, D). These findings suggest that TgUAE1 plays a crucial role in maintaining mitochondrial homeostasis, also linked to its ubiquitin activation site.

TgUAE1 is crucial in regulating specific lysine-linked polyubiquitin chains

To further corroborate the previously described in vivo and in vitro evidence for ubiquitin-activating enzyme activity, the overall levels of ubiquitinated proteins in the cKD-TgUAE1 strain were compared under ATc and non-ATc treatment conditions. Following 4 days of ATc treatment, a significant reduction in the detectable levels of ubiquitinated proteins was observed and a decrease in TgUAE1 expression (Fig. 7A).

To further investigate the role of TgUAE1 in regulating the formation of K48- and K63-linked polyubiquitin chains, the two most prevalent polyubiquitin chains in mammalian cells, we performed WB analysis (Fig. 7B, D). The results showed a marked impairment in the formation of both polyubiquitin chains in the cKD-TgUAE1 strain upon TgUAE1 depletion compared to the parental strain. While the levels of both polyubiquitin chains were restored through complementation with wild-type TgUAE1, the C634S mutation in TgUAE1 failed to rescue this effect (Fig. 7B, C). Statistical analysis of the K48-linked ubiquitination levels (Fig. 7C) showed significant differences, with the cKD-TgUAE1 strain exhibiting lower levels compared to parental strain ($^*p < 0.05$). Similarly, for K63-linked ubiquitination, the cKD-TgUAE1 strain also showed significant reductions in polyubiquitin levels (Fig. 7D), which were not rescued by the C634S mutation (Fig. 7E, $^*p < 0.05$). These results indicate that TgUAE1 regulates ubiquitination at K48- and K63-linked polyubiquitin sites in *T. gondii*, and its function relies heavily on the catalytic activity of the ubiquitin-activating site.

Transcriptome profiling of TgUAE1 downregulation in *T. gondii*

To gain an in-depth understanding of the effects of TgUAE1 on the lytic cycle and mitochondrial integrity, transcriptomes were constructed based on the cKD-TgUAE1 strain with and without ATc treatment. The resulting dataset comprised 8637 genes mapped to the *T. gondii* genome. Within this dataset, 940 differentially expressed genes (DEGs; up/down ratio, 878:62) were identified at statistically significant levels ($\log_2 R \leq -1$ or ≥ 1, $p < 0.05$), accounting for 10.88% of the entire genome (Fig. 8A, Supplementary Data 2-1).

Gene ontology (GO) analysis revealed significant enrichment of 350 DEGs with an up/down ratio of 332:18 across 29, 20, and 27 GO terms belonging to three functional classes (Supplementary Data 2-2). Figure 8B illustrates the main GO terms within the cellular component, molecular function, and biological process categories. A total of 110 DEGs were enriched in the cellular component category, with significant enrichment in membrane, kinesin complex, peroxisome, and rhoptry. In the molecular function category, 135 DEGs were primarily involved in ATP binding, ATPase activity, microtubule motor activity, kinase activity, and transferase activity. The biological process category, with 105 DEGs, was enriched for processes such as microtubule-based movement, oxidation-reduction processes, and intracellular signal transduction. The enrichment in these terms further supports the observation that TgUAE1 knockdown disrupts key biological functions, leading to the observed defects in gliding, invasion, egress, and intracellular proliferation.

Kyoto Encyclopedia of Genes and Genomes (KEGG) analysis identified 87 DEGs (up/down ratio, 81:6) enriched in 23 pathways (Supplementary Data 2-3). Among these, the main enriched pathways are shown in Fig. 8C. Notably, the peroxisome, purine metabolism, cAMP signaling pathway, and fatty acid biosynthesis and metabolism pathways exhibited significant enrichment in upregulated genes. The findings from the KEGG pathway analysis suggest that TgUAE1 is involved in regulating multiple cellular processes, including signaling pathways, lipid metabolism, and cellular stress responses.

To validate the reliability of the transcriptome, 7 genes were randomly selected from the pool of 940 differentially expressed genes for RT-qPCR analysis. The results demonstrated significant downregulation or upregulation in the transcripts of these 7 genes (Fig. 8D), consistent with the transcriptome data. Further analysis of the differentially expressed genes revealed a significant upregulation of SAG-related sequence proteins and BAG1 (bradyzoite antigen gene 1), suggesting that *T. gondii* may be undergoing a transition between lifecycle stages or responding to changes in the host environment, leading to adjustments in its biological state. Additionally, the analysis of stress-related genes revealed the presence of oxidative stress (2 DEGs), with a predominant response related to ER stress (5 DEGs) (Supplementary Data 2-4). Previous evidence suggests that inhibition of UAE1 induces robust ER stress[26,27], as highlighted by our GO and KEGG pathway analysis, we further investigated the transcriptional response of ER stress-related genes in *T. gondii* through RT-qPCR to better understand the underlying molecular mechanisms. To validate this hypothesis, the transcription of 6 genes reported to be upregulated during ER stress in *T. gondii*[28] was compared between cKD-TgUAE1 parasites with and without ATc treatment by RT-qPCR. These genes included *Tgpuf* (TGGT1_260600), glycosyltransferase (TGGT1_207070), SAG-related sequence SRS49D (*Tgsag2c*, TGGT1_207160), *Tgderlin1* (TGGT1_217160), hypothetical

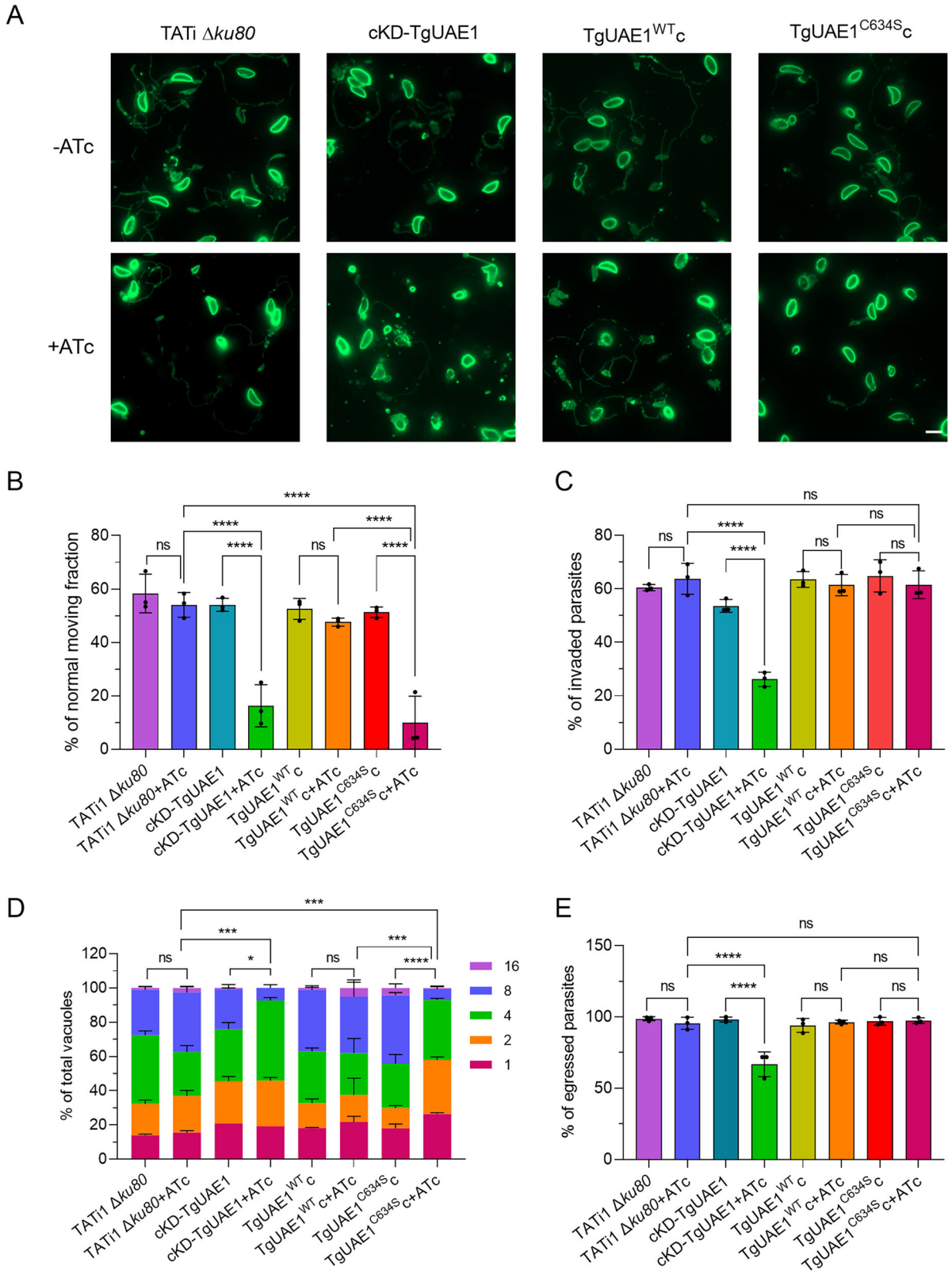

protein (TGGT1_277230), and trehalose-phosphatase (TGGT1_297720). Notably, the bradyzoite-specific surface antigen *Tgsag2c* (TGGT1_207160) was significantly upregulated in response to ER stress[28]. The results consistently demonstrated significant upregulation in ATc-treated cKD-TgUAE1 parasites (Fig. 8E), aligning with the transcriptome data.

Taken together, these results suggest that TgUAE1 depletion induces ER stress in *T. gondii*, which could potentially trigger a transition to a bradyzoite-like state. This is supported by the upregulation of bradyzoite-specific antigens, including *Tgsag2c*, in response to ER stress. The findings imply that stress caused by TgUAE1 knockdown leads to alterations in

Fig. 5 | The effect of TgUAE1 on the lytic cycle in cKD-TgUAE1, TgUAE1^{WT}c, and TgUAE1^{C634S}c lines compared to TATi1 Δ*Ku80* with or without ATc treatment. **A** The effect of TgUAE1 on the gliding ability of *T. gondii* was examined using a fluorescence microscope with TgSAG1 antibody staining. Scale bar = 5 μm. **B** The gliding ability was determined by calculating the ratio of tachyzoites exhibiting slippage to the total number of parasites. Data are presented as means ± SD from three biological replicates, with at least 100 parasites per line counted. **C** The invasion percentage was determined by calculating the ratio of intracellular tachyzoites to the total number of parasites. Data are presented as means ± SD from three biological replicates, with at least 100 parasites per line counted. **D** The intracellular proliferation ability was assessed by determining the proportion of vacuoles containing different numbers of parasites relative to the total number of vacuoles. Data are presented as means ± SD from three biological replicates, with at least 100 vacuoles per line counted. **E** The egression percentage was determined by calculating the ratio of ruptured vacuoles to the at least 100 vacuoles. Data are presented as means ± SD from three biological replicates. Statistical significance was determined using a one-way ANOVA (ns $p > 0.05$, *$p < 0.05$, ***$p < 0.001$, ****$p < 0.0001$).

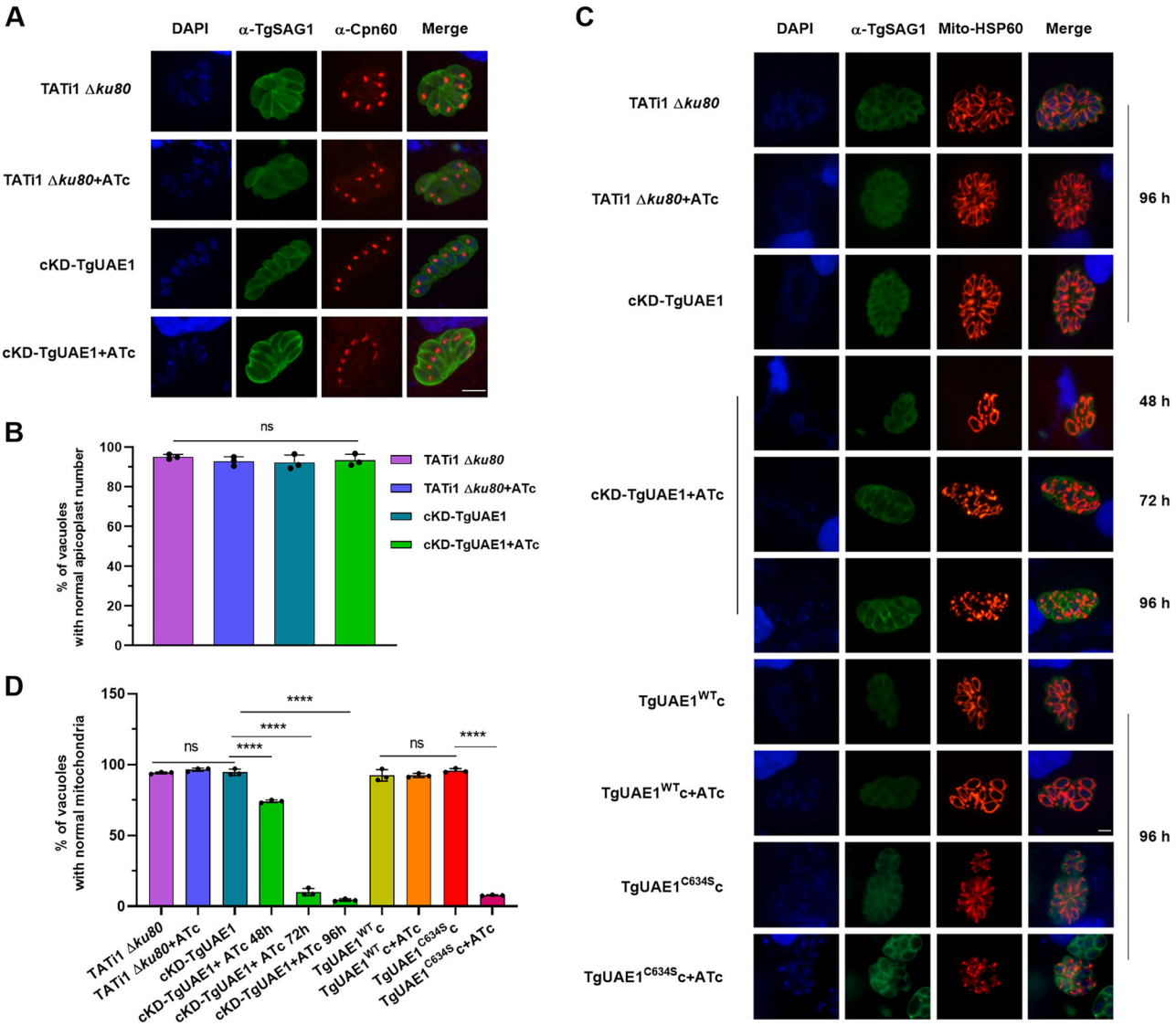

Fig. 6 | The effect of TgUAE1 on the morphology of subcellular organelle in *T.gondii* tachyzoites. **A** The morphological changes of the apicoplast were observed by IFA using an antibody against α-Cpn60 (red) in TATi1 Δ*Ku80* and cKD-TgUAE1 parasites with or without ATc treatment for 96 h (scale: 5 μm). Parasites were also labeled with DAPI (blue) and α-TgSAG1 (green). **B** Statistical analysis showing the percentage of vacuoles with normal apicoplasts within parasitophorous vacuoles (PVs). Data are presented as means ± SD from three biological replicates, and statistical significance was determined using a one-way ANOVA (ns $p > 0.05$). **C** Mitochondrial morphological changes were observed by IFA in TATi1 Δ*Ku80*, cKD-TgUAE1, TgUAE1^{WT}c and TgUAE1^{C634S}c strains, with or without ATc treatment. A transiently transfected Mito-Hsp60-RFP plasmid (red) was used to label mitochondria, and parasites were stained with DAPI (blue) and an antibody against α-TgSAG1 (green). ATc treatment was applied for 48, 72, or 96 h, as indicated (scale: 5 μm). **D** Statistical analysis showing the proportion of vacuoles with normal mitochondria within PVs. Data are presented as means ± SD from three biological replicates, and statistical significance was determined using a one-way ANOVA (ns $p > 0.05$, ****$p < 0.0001$).

T. gondii's biological state, promoting the conversion from tachyzoite to bradyzoite. This transition is likely a part of the parasite's response to stress conditions and environmental changes, highlighting the role of TgUAE1 in maintaining cellular homeostasis and regulating the life cycle of *T. gondii*.

Effect of TgUAE1 downregulation on the protein expression profiles of *T. gondii*

To comprehensively understand the mechanism and regulatory network of TgUAE1-mediated in *T. gondii*, the TATi1 Δ*ku80* strain was used as the control group, with the cKD-3HA-TgUAE1 strain serving as the

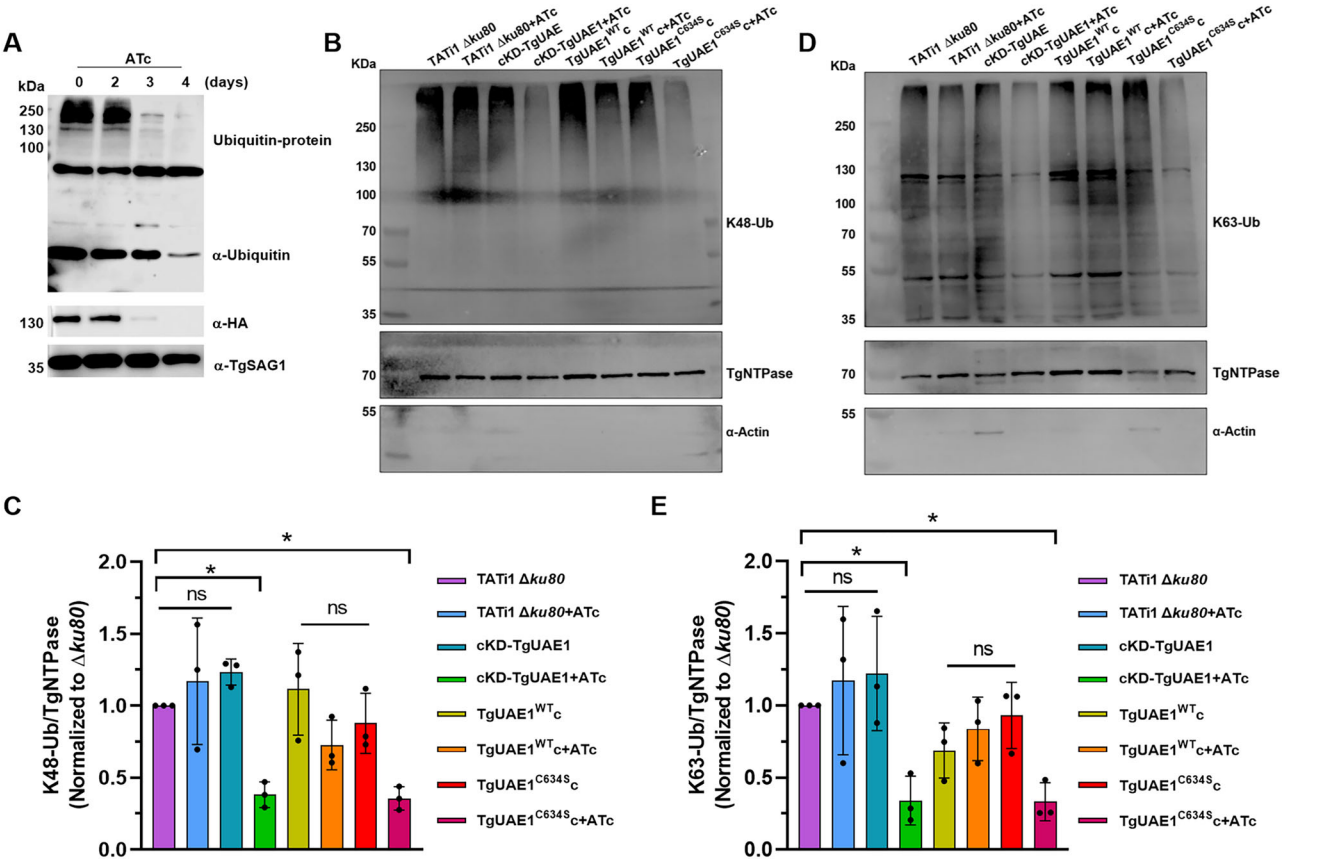

Fig. 7 | Effect of TgUAE1 on the ubiquitination modification in *T. gondii*. **A** The ubiquitination level in the cKD-TgUAE1 strain under 0, 2, 3, or 4 days of ATc treatment was assessed by WB using an α-ubiquitin antibody. The expression of TgUAE1 protein was evaluated using an α-HA antibody, with an α-TgSAG1 antibody employed as an internal control. **B** The level of K48-linked ubiquitination in TATi1 Δ*Ku80*, cKD-TgUAE1, TgUAE1^{WT}c, and TgUAE1^{C634S}c parasite lines with or without ATc treatment were detected by WB using a K48-specific anti-ubiquitin antibody. TgNTPase served as the *T. gondii* internal control, and α-actin was used as the host HFF cell internal control. **C** Quantification of K48-linked ubiquitination relative to TgNTPase levels, normalized to the TATi1 Δ*Ku80* group. Data are presented as mean ± SD from three independent experiments. Statistical significance was determined using a one-way ANOVA (*$p < 0.05$, ns $p > 0.05$). **D** The level of K63-linked ubiquitination in TATi1 Δ*Ku80*, cKD-TgUAE1, TgUAE1^{WT}c, and TgUAE1^{C634S}c parasite lines with or without ATc treatment were detected by WB using a K63-specific anti-ubiquitin antibody. TgNTPase served as the *T. gondii* internal control, and α-actin was used as the host HFF cell internal control. **E** Quantification of K63-linked ubiquitination relative to TgNTPase levels, normalized to the TATi1 Δ*Ku80* group. Data are presented as mean ± SD from three independent experiments. Statistical significance was determined using a one-way ANOVA (*$p < 0.05$, ns $p > 0.05$).

experimental group. Both strains were treated with ATc for 72 h, followed by cell lysis and collection of cellular precipitates. Protein extraction was performed via ultrasonic disruption and subsequent trypsin digestion, Proteomic and ubiquitination proteomic analysis were conducted using liquid chromatography-mass spectrometry (LC-MS), with each sample analyzed in duplicate. Proteomic analysis identified a total of 3608 proteins, of which 3308 proteins were quantified. Following the downregulation of TgUAE1, we identified 520 differentially expressed proteins (DEPs), including 195 upregulated proteins and 325 downregulated proteins (Fig. 9A, Supplementary Data 1–3). Notably, significant differential expression was observed in the ER (33 DEPs) and mitochondria (28 DEPs), indicating that these organelles might be affected by TgUAE1 knockdown (Supplementary Data 3-1). These findings further highlight the crucial role of TgUAE1 in maintaining cellular homeostasis in *T. gondii*. Additionally, the localization analysis revealed that proteins were enriched in key cellular structures, such as ribosomes (25 DEPs), dense granules (15 DEPs), and rhoptries (28 DEPs). Ribosomes are crucial for protein synthesis, dense granules are involved in secreting virulence factors during host invasion, and rhoptries play a key role in host cell invasion and immune evasion.

To investigate the downstream substrate proteins of TgUAE1 and the biological pathways it may regulate, we performed GO analysis on these DEPs (Fig. 9B, Supplementary Data 3-2). The results showed that DEPs were predominantly localized to sub-cellular organelles, with many having protein binding capacity, organic cyclic compound binding capacity, transferase enzyme activity, and catalytic enzyme activity. These proteins were mainly involved in cellular component biogenesis, various metabolic processes, and stress responses. KEGG pathway analysis revealed that, following TgUAE1 knockdown, DEPs were most enriched in pathways related to ribosomes, proteasomes, glucagon signaling, and glycolysis/gluconeogenesis (Fig. 9C, Supplementary Data 3-3). Based on these findings, we hypothesize that TgUAE1 may influence *T. gondii* biological processes through two mechanisms. First, regulation of protein synthesis: TgUAE1 may regulate the expression of ribosomal components, thereby affecting the synthesis of substrate proteins and leading to the downregulation of certain substrate proteins. Second, regulation of protein degradation: TgUAE1 knockdown may inhibit the degradation of specific substrate proteins via the ubiquitin-proteasome pathway, resulting in the upregulation of these proteins (Supplementary Data 3-4).

These results collectively underscore the pivotal role of TgUAE1 in regulating critical cellular processes such as protein synthesis, degradation, and organelle function, which are essential for maintaining homeostasis and optimal biological function in *T. gondii*

Effect of TgUAE1 downregulation on *T. gondii* ubiquitination pattern

Proteomic analysis revealed the identification of 3608 proteins, of which 3308 were subjected to quantitative analysis. Among these, 716 out of 1596

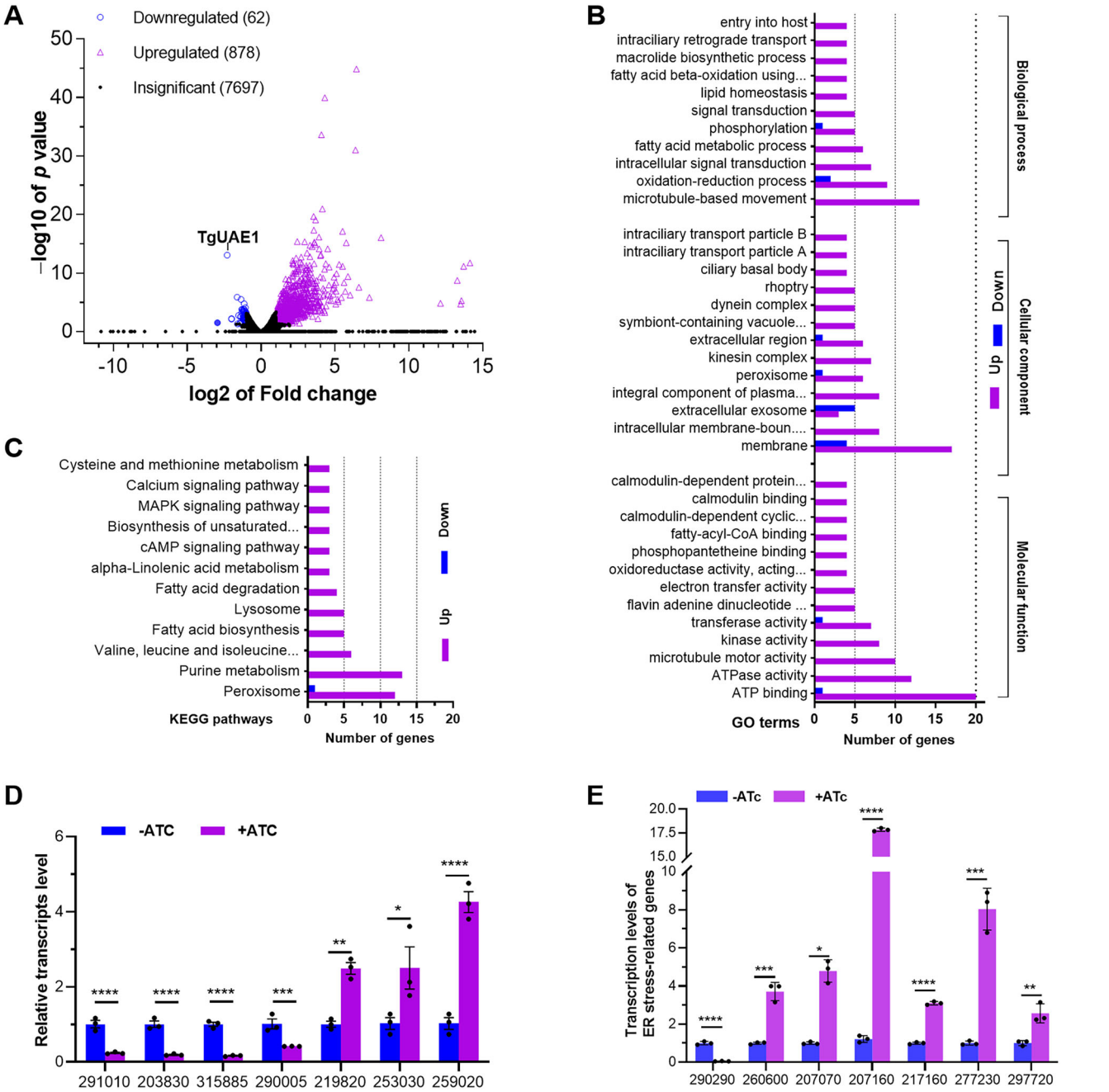

Fig. 8 | Profound effect of TgUAE1 conditional knockdown on the genomic expression of *T. gondii*. **A** Distributions of $\log_2$ R and *q* values for all genes identified in the transcriptomes generated from cKD-TgUAE1 strains treated with ATc or DMSO. Differentially expressed genes (DEGs) are those significantly downregulated ($\log_2 R \leq 1$) or upregulated (($\log_2 R \geq 1$) with a level of *q* value < 0.05. Genes with $-1 \leq \log_2 R \leq 1$ or $q \geq 0.05$ when $\log_2 R \leq -1$ or ≥1 are considered insignificantly affected. **B, C** Counts of DEGs significantly enriched ($p < 0.05$) in three function classes (main GO terms shown) and the top 12 KEGG pathways. **D** RT-qPCR validation of seven randomly selected genes from the 940 DEGs. **E** The transcription levels of TgUAE1 (TGGT1_290290) and six genes with significant changes during ER stress were validated by RT-qPCR under treatment with ATc or DMSO. Data are presented as means ± SD from three biological replicates, and statistical significance was determined using a *t* test (*$p < 0.05$; ***$p < 0.001$; ****$p < 0.0001$).

ubiquitinated proteins and 1697 out of 4495 ubiquitination sites were specifically identified for quantitative analysis (Fig. 10A, Supplementary Data 4-1). Among them, 55 proteins displaying differential ubiquitination (up/down ratio of 14:41), and 63 sites exhibiting differential ubiquitination on proteins (DUPs: up/down ratio of 17:46) at a significant level (Fold Change, FC > 1.5 or < 1/1.5, CV < 0.1) (Fig. 10B).

GO analysis revealed that, following TgUAE1 knockdown, a total of 20 DUPs were enriched in multiple GO terms (Fig. 10C, Supplementary Data 4-2). In terms of biological processes, DUPs were predominantly enriched in cellular metabolic processes, organic substance metabolic processes, primary metabolic processes, and biosynthetic processes, suggesting that TgUAE1 may influence cellular functions by regulating these metabolic and biosynthetic pathways. DUPs enriched in processes such as cell cycle, cell motility, response to stress, and cell division, implying that TgUAE1 knockdown may affect cellular proliferation, division, motility, and stress response functions. Molecular function analysis revealed that the DUPs were primarily associated with protein binding, hydrolase activity, and organic cyclic compound binding, suggesting their potential role in cellular signal transduction and metabolic processes. In terms of cellular components, both upregulated and downregulated proteins were enriched

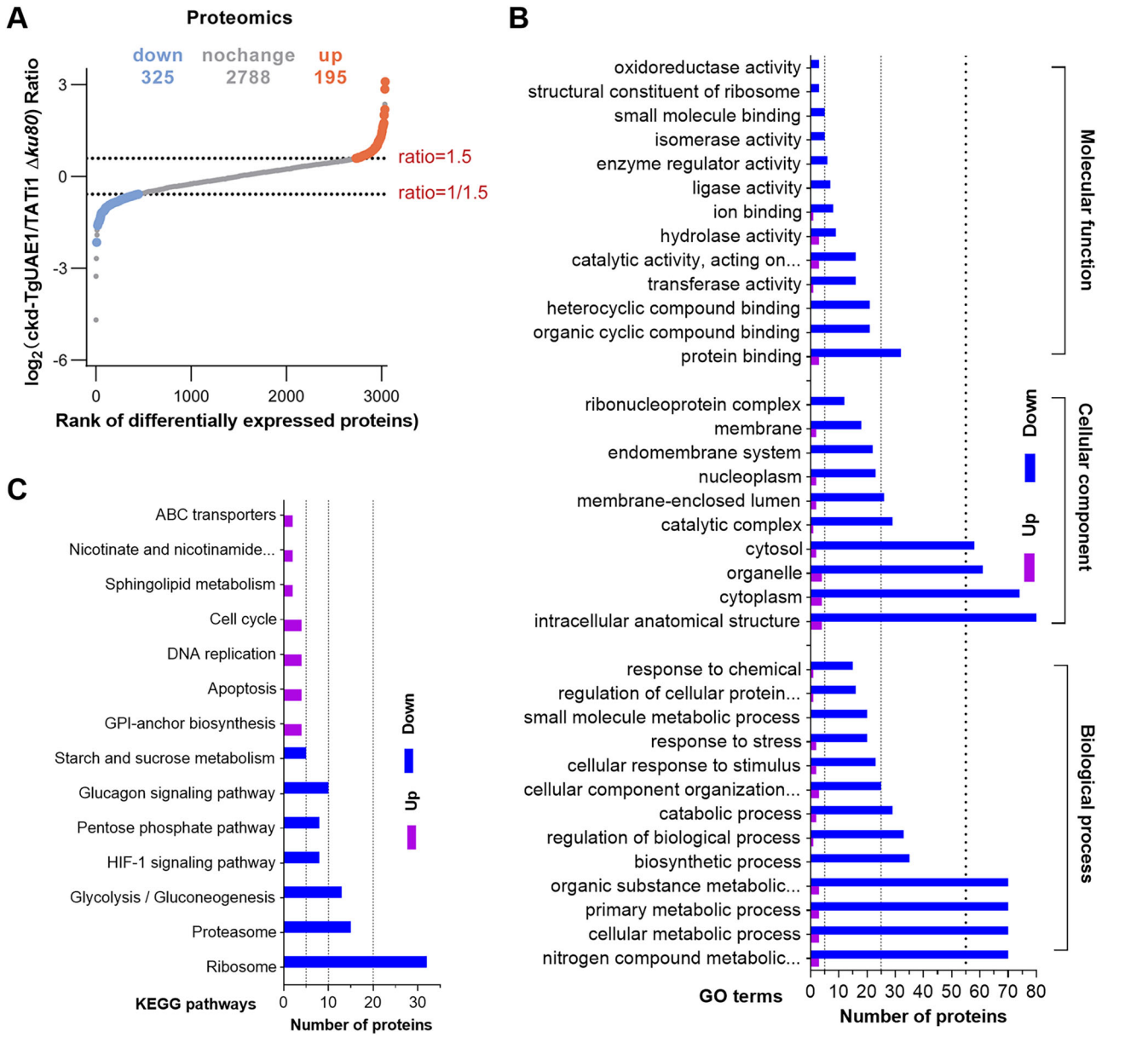

Fig. 9 | Proteomic analysis of TgUAE1 conditional knockdown in *T. gondii*. **A** The $\log_2$(cKD-TgUAE1/TATi1 Δ*ku80*) ratio for differentially expressed proteins. The plot shows 325 downregulated, 2788 unchanged, and 195 upregulated proteins. The dotted lines indicate the thresholds for proteins with a fold change greater than 1.5 (upregulated, red) or less than 1/1.5 (downregulated, blue). **B** GO term enrichment analysis of differentially expressed proteins, categorized into Molecular Function, Cellular Component, and Biological Process. The number of proteins enriched in each term is shown on the x-axis. **C** KEGG pathway enrichment analysis showing the significant pathways associated with the differentially expressed proteins.

in the cytoplasm, cytosol, and organelles, further indicating their involvement in the regulation of basic cellular functions and structures. According to the subcellular classification of the differentially ubiquitinated proteins (Supplementary Data 4-1), the majority of proteins were localized to the cytosol (12 DUPs) and nucleus (12 DUPs). Notably, significant differentially ubiquitinated proteins observed in the ribosomes (7 DUPs), ER (6 DUPs), rhoptries (4 DUPs), dense granules (2 DUPs), and mitochondria (1 DEPs), indicating that these organelles might be affected by TgUAE1 knockdown. Among the DUPs, the ubiquitination of ATG8, a key autophagy-related protein[29], was found to be significantly downregulated. While ATG8 is commonly associated with autophagy, its reduction in ubiquitination may reflect disturbances in autophagic processes, including those potentially related to mitochondrial quality control. The KEGG pathways analysis indicates that TgUAE1-mediated ubiquitination affects a wide range of cellular processes (Fig. 10D, Supplementary Data 4-3). These include translation, cell growth and death, metabolism, signal transduction and folding, sorting and degradation pathways. These findings suggest that TgUAE1-mediated ubiquitination plays a critical role in regulating various cellular processes, including metabolism, protein synthesis, stress responses, and organelle function (Supplementary Data 4-4), thereby maintaining cellular homeostasis and supporting the efficient biological activities required for *T. gondii* survival and proliferation.

Discussion

The process of ubiquitylation, a widespread post-translational modification in eukaryotes, plays a pivotal role in protein regulation. Our understanding of the *T. gondii* ubiquitination system remains incomplete, and distinct differences in proteasome localization have been observed between *T. gondii* and mammals. While mammalian proteasomes are typically present in the cytoplasm and nucleus, *T. gondii* proteasomes are exclusively cytoplasmic[30]. Recently, a ubiquitin-activating enzyme, PfUAE1, with canonical E1 activity, was identified in *P. falciparum*[17]. However, the presence and

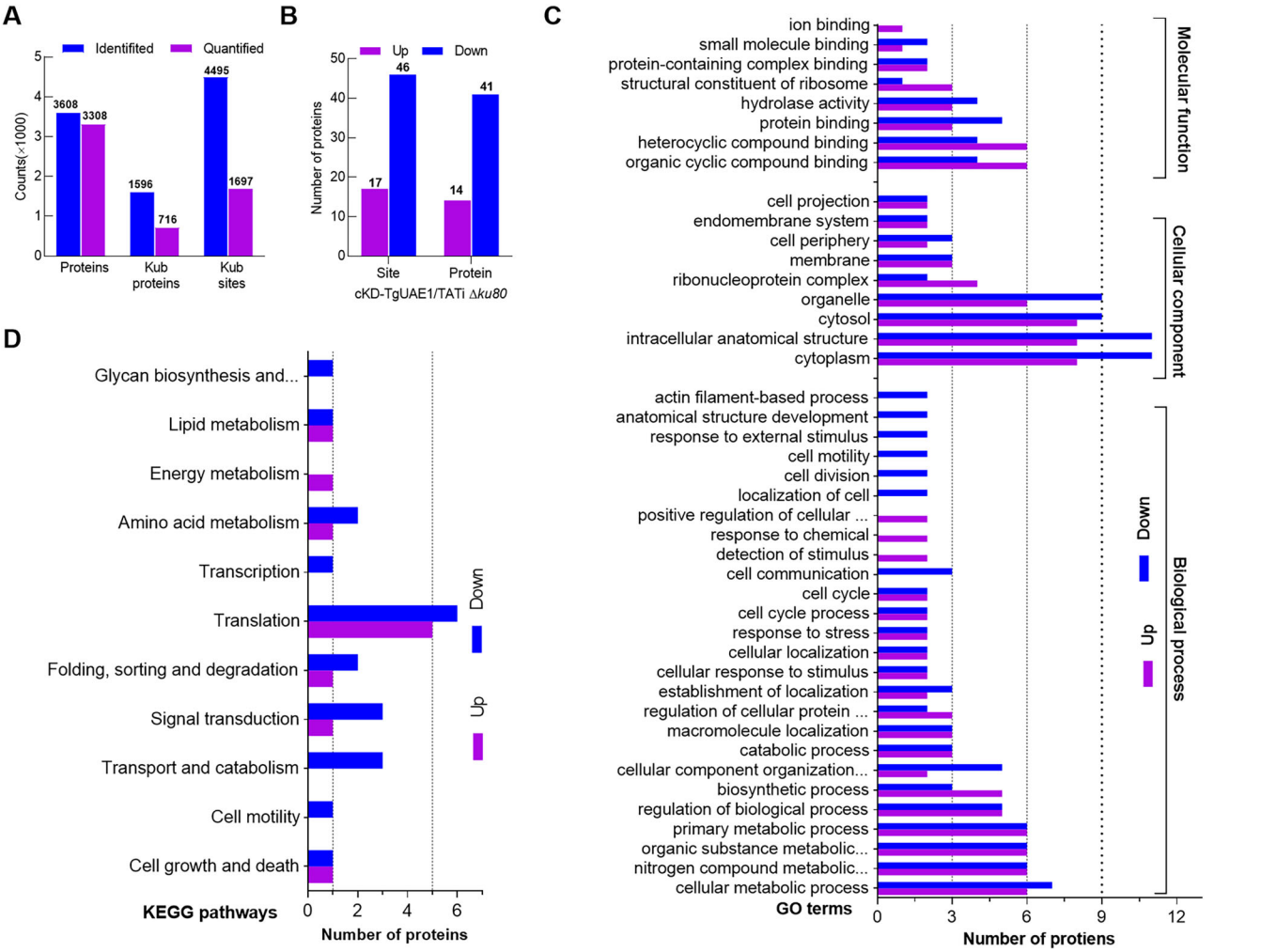

Fig. 10 | Profound effect of TgUAE1 conditional knockdown on ubiquitination quantitative proteomics of *T. gondii*. **A** The numbers of total proteins, ubiquitinated proteins, and ubiquitinated sites were determined and quantified in cKD-TgUAE1 compared with TATi1 Δ*Ku80* strain under ATc treatment. **B** The numbers of differentially ubiquitinated proteins and protein sites quantified between cKD-TgUAE1 and TATi1 Δ*Ku80* strain under ATc treatment. **C** GO term enrichment analysis showing the biological processes and molecular functions associated with differentially expressed ubiquitinated proteins. The bar chart displays the number of proteins enriched in the respective GO terms, where blue indicates downregulated proteins and purple indicates upregulated protein. **D** The counts of differentially ubiquitinated proteins significantly enriched in KEGG pathways.

functional implications of E1 enzymes in *T. gondii* regarding ubiquitination regulation remains elusive. Our study is the fist time to identify TgUAE1 (TGGT1_290290) as a canonical E1 enzyme, which plays a crucial role in the lytic cycle and homeostasis of *T. gondii*, with its pleiotropic effects discussed below.

In the present study, TAK-243, a specific inhibitor targeting UAE1, which has previously been limited to *P. falciparum* in apicomplexans[17], was investigated. The inhibitory effect of TAK-243 on TgUAE1 in *T. gondii* was unclear. The inhibitor enhances the stability of the target protein by binding to a specific site in the PfUAE1 protein, thereby mitigating its susceptibility to degradation under changing external conditions, such as elevated temperatures[20]. Our results show that TAK-243 effectively inhibits TgUAE1 in *T. gondii*, significantly reducing parasite proliferation, although the TI was relatively small (1.15), suggesting that the drug's efficacy against the parasite and its toxicity to host cells are closely balanced. Moreover, this study is the first to confirm that TAK-243 can effectively inhibit the ubiquitin pathway in *T. gondii*, making it a valuable tool for related studies.

A ubiquitination system unique to apicomplexans was identified within the apicoplast, which includes $TgE1_{AP}$[15], $TgE2_{AP}$[31], and $TgE3_{AP}$[32]. This system crucial in apicoplast protein import, with $TgE1_{AP}$ (TGME49_314890) recognized as an E1 enzyme[15]. TgUAE1, while sharing conserved active sites with ScUba1 and HsUba1, differs from $TgE1_{AP}$ by the absence of 642 amino acids in its N-terminal region. Moreover, the knockdown of TgUAE1 does not significantly affect the morphology or homeostasis of the apicoplast, highlighting differences from $TgE1_{AP}$. Although the TGGT1_212100 encoding product has been identified as involved in ubiquitin-like modification in *T. gondii*, and referred to as TgUba1, it functions solely as a ubiquitin-like activator enzyme. It lacks the characteristic features of canonical E1 enzymes[16]. Protein ubiquitination plays a crucial role in the cell cycle of *T. gondii*, encompassing over 500 proteins that undergo ubiquitin modification at nearly 1000 sites, with about 35% directly involved in regulating the cell cycle[33,34]. The lytic cycle of cKD-TgUAE1 and $TgUAE1^{C634S}$c mutants was suppressed, indicating a pivotal role of TgUAE1 in post-infection cellular events crucial for growth. In Apicomplexa, gliding motility is driven by an actomyosin motor anchored to inner membrane complex (IMC), and ubiquitination of myosin proteins may be important for rearrangement of the cytoskeleton or regulation of motor function. Our transcriptomic analysis identified dozens of dysregulated genes involved in motility, along with 52 SAG-related genes and the BAG1 gene (Supplementary Data 2–4). Specifically, the DUPs related to motility, such as actin depolymerizing factor (ADF) and several myosins (myosinA/F/H), showed significant changes in ubiquitination in response

to TgUAE1 knockdown (Supplementary Data 4-4). TgADF plays a crucial role in maintaining actin dynamics, as evidenced by the increased stabilization of F-actin and subsequent disruption of motility following its suppression[35,36]. In particular, myosin complexes, such as myosin F, are involved in the movement of the parasite and can directly affect the gliding ability. The downregulation of these proteins could explain the observed defects in parasite motility and tachyzoite proliferation in TgUAE1-depleted parasites. The identification of DUPs associated with translation-related proteins, such as the eukaryotic initiation factor (TGGT1_216260), highlights the role of TgUAE1 in regulating protein translation. Since translational control is critical for proper parasite development, TgUAE1 depletion may lead to disruptions in this process. Furthermore, this depletion could alter the transcriptional regulation of stress response and cell cycle-related genes, ultimately contributing to the defects observed in *T. gondii* biology. Notably, while TgUAE1 knockdown abolished all lytic functions, including gliding motility, invasion, proliferation, and egress, the C634S mutation specifically impaired intracellular proliferation and gliding persistence, while preserving invasion and egress. Parasite invasion and egress are generally powered by a gliding motility. However, during invasion, a ring-shaped complex of F-actin, ARP2/3 and cortactin is observed in the host cell at the site of the moving junction[37]. This actin remodeling is thought to anchor the parasite to the host cell and facilitate deformation of the host cell membrane during invasion. In cases where gliding motility is severely impaired, such as in TgmyosinA-deficient parasites, this actin remodeling appears to be even more critical[38]. The C634S mutation may exploit this mechanism to facilitate invasion despite impaired motility. On the other hand, members of the Apicomplexa phylum possess specialized secretory organelles such as rhoptries, micronemes, and dense granules that release key factors in a regulated, timely manner at the apical end. These factors play crucial roles in parasite motility, host cell invasion, egress, and the manipulation of host cellular functions[39,40]. The ubiquitination proteomic analysis of TgUAE1 knockdown revealed that only the dense granule proteins GRA2 and GRA14 exhibited changes in ubiquitination (Supplementary Data 4-4), suggesting that while TgUAE1 is involved in these processes, its role may be limited. The C634S mutation likely retains sufficient residual enzymatic activity to support the transient demands of invasion and egress. It is also possible that TgUAE1's contribution to invasion and egress extends beyond its enzymatic activity. Regions outside the catalytic site, such as the UBA domain and C-terminal ubiquitin-fold domain, may mediate interactions with parasite-specific pathways or host cell components. These interactions could trigger microneme exocytosis or perforin activation during invasion and egress, bypassing the need for ubiquitination modifications. CDPK3, for instance, is known to phosphorylate the myosin motor and regulate calcium-dependent microneme secretion during egress[41,42]. Future studies, including combinatorial mutations targeting potential active sites along with enzymatic activity assays, will be essential for elucidating the precise role of Cys634 in TgUAE1 function. Additionally, exploring the structural and functional domains beyond the catalytic site, through truncation mutagenesis and interaction mapping, will provide valuable insights into their contributions to the *T. gondii* life cycle.

Experiments have shown that the absence of TgUAE1 also inhibited the intracellular proliferation of tachyzoites. The phenotype score associated with the TgUAE1 encoding gene (-4.25) was significantly lower than most genes in ToxoDB, suggesting that TgUAE1 may have more severe effects in *T.gondii*. This is consistent with ubiquitination quantitative proteomics results, where DEPs and DUPs were mainly involved in the biogenesis, metabolism and stress response. Although the specific processes most critical for *T. gondii* growth are not yet known, this area requires further investigation. However, it is worth noting that these processes indeed impact *T.gondii* homeostasis. The most well-known function of ubiquitylation is targeting proteasome degradation of proteins[43]. Misfolded proteins transported through the ER are subjected to polyubiquitination and subsequent degradation, constituting the ERAD process[44]. Inhibiting this modification results in a continuous buildup of numerous unfolded and misfolded proteins, leading to increased ER stress and subsequent impairment of subcellular organelle structure and function[45–47]. The unfolded protein response (UPR) identifies misfolded proteins in the ER, while the heat shock response (HSR) addresses cytoplasmic misfolded proteins, facilitating their correct folding and degradation[48]. Ubiquitination of the Hsp70 protein is important in facilitating protein folding and maintaining protein homeostasis[49,50]. In our study, the transcriptional levels of ER stress-related genes were significantly upregulated after TgUAE1 knockdown. Furthermore, ubiquitination quantitative proteomics analysis found a downregulation in the ubiquitination modification level of Hsp70, eukaryotic initiation factor eIF5A involved in ER stress, and several ribosomal proteins involved in the cell cycle. Mitochondrial fragmentation also indicated that *T. gondii* homeostasis was seriously affected. Previous studies have demonstrated that decreased ubiquitin levels can alter mitochondria morphology[51]. Recent proteomic analyses of mitochondria from *T. gondii* ME49 strains and mammalian cells identified UAE1[52,53], suggesting an important role for this protein in maintaining mitochondrial structure and function. However, it is unclear whether this is a direct or secondary effect of the lack of E1 activity in the cytosol for normal ubiquitination and proteasomal degradation, warranting further investigation. The ER is a key organelle for cell function and metabolic adaptation. Dysfunction of the ER, known as "ER stress," is a fundamental characteristic of metabolic disorders[54]. In the TgUAE1 knocked-down strain, differentially ubiquitinated proteins mainly focused on enzyme activity (transferase, kinase, ATPase), membrane components, oxidation-reduction signal transduction, response to stress, intracellular metabolism, and other processes, reflected in translation, transcription, and metabolic pathways. Our study demonstrated that TgUAE1 deficiency leads to losing control of genome-wide expression regulation, disrupting homeostasis and inhibiting *T. gondii* growth and development.

Conclusions

In conclusion, this study identifies TgUAE1 as a canonical ubiquitin-activating enzyme 1 in *T. gondii* and confirms its enzymatic activity both in vitro and in vivo. Our findings demonstrate that TgUAE1 is essential for proper ubiquitination processes, as its deficiency leads to significant transcriptional changes and a reduction in ubiquitination, indicating an impact on protein turnover. While TgUAE1 appears to play a crucial role in regulating genome-wide expression, future studies should address whether residual enzymatic activity persists in the C634S mutant and explore potential non-catalytic roles of TgUAE1 in parasite biology. Further investigation into its involvement in environmental sensing, immune evasion, and domain-specific interactions will deepen our understanding of ubiquitination's role in *T. gondii* pathogenesis. Although TgUAE1 is a conserved enzyme across eukaryotes, understanding its function in the context of *T. gondii* provides insights into the parasite's biology and could inform future research on potential therapeutic targets. This study lays the groundwork for further exploration of ubiquitination in *T. gondii* and its implications for parasite survival and pathogenesis.

Materials and methods

Cell cultivation and parasite culture

The tachyzoites of *T. gondii* strain RH-2F[24], RH Δ*Ku80*, and TATi1 Δ*Ku80*[55,56], along with their transgenic derivatives, were continuously cultured in monolayers of human foreskin fibroblasts (HFF, ATCC, SCRC1041) at 37 °C with 5% CO_2. The culture medium used was Dulbecco's Modified Eagle Medium (DMEM, Gibco, Cat#11995-065) supplemented with 10% fetal bovine serum (Gibco, Cat#10099-141) and 0.5 mg/ml penicillin-streptomycin-glutamine (Gibco, Cat#10378-016).

Recognition and bioinformatic analysis of TgUAE1 homologs

The UAE1 sequences of *S. cerevisiae* (CAA82055) were used to query the *T. gondii* genomic database at ToxoDB (http://www.toxodb.org). Phylogenetic analysis of the E1 family proteins from *T. gondii, S. cerevisiae, H. sapiens*, and *D. rerio* was conducted using the Neighbor-Joining method in MEGA7.0 software[57]. The amino acid sequences of UAE1 from various

species were aligned using GeneDoc[58]. The prediction model for the structure of TgUAE1 was generated using RaptorX (http://raptorx.uchicago.edu/)[59]. Structure alignment and docking images were obtained using PyMoL2.4 (Schrodinger, LLC), with the structure of ScUAE1 retrieved from the Protein Data Bank (PDB, 5tr4).

Plasmid constructions and parasite transfections

All the primers used in the present study are listed in Supplementary Data 1.

To introduce 3HA tags at the 3' end of the endogenous *Tguae1*, a genomic DNA sequence located 1478 bp upstream of the stop codon of *Tguae1* was amplified using primers U1-F/R and cloned into the pLIC-DHFR-3HA vector[60]. 100 μg *Blp*I-linearized recombinant plasmid pLIC-DHFR-TgUAE1-3HA was transfected into 1×10^7 RH Δ*Ku80* parasites. Positive monoclonal strains were selected by adding pyrimethamine 24 h post-transfection.

For conditional knockdown of TgUAE1 using the TATi1-ATc strategy[56], a 1500 bp fragment starting from the initiation codon of the TgUAE1 was amplified from genomic DNA using primers U2-F/R, which includes an N-terminal 3HA tag. The fragment was then cloned into the *Avr*II and *Not*I sites within the pTetO7Sag4-3HA-TgATG7 vector[29]. The resulting plasmid, pTetO7Sag4-3HA-TgUAE1, was linearized by *Eco*RV and transfected into TATi1 Δ*Ku80* parasites. Positive monoclonal strains were selected by pyrimethamine screening and limiting dilution, followed by PCR confirmation using primers P1/P2-F/R to validate correct integration at the recombined locus. PCR-confirmed positive clones underwent further verification via WB and qRT-PCR to determine the downregulation efficiency of TgUAE1 after treatment with 0.5 μg/ml ATc for 4 days, and were designated as cKD-TgUAE1.

To complement a constitutively expressed wild-type TgUAE1 in the cKD-TgUAE1 strain, the full-length coding sequence of TgUAE1 was amplified using primers U3-F/R and inserted into the *Aat*II and *Eco*RV sites of the pTub-3FLAG-TgATG7-CAT vector[29], generating the plasmid pTub-3FLAG-TgUAE1^{WT}-CAT. To complement a constitutively expressed TgUAE1^{C634S} mutant, the sequence corresponding to the 'C634' residue in pTub-3FLAG-TgUAE1^{WT}-CAT was mutated to serine using Q5® Site-Directed Mutagenesis Kit (New England Biolabs, E0554S) with primers U4-F/R. A total of 100 μg of *Mss*I-linearized pTub-3FLAG-TgUAE1^{WT}-CAT and pTub-3FLAG-TgUAE1^{C634S}-CAT were transfected into cKD-TgUAE1 parasites, respectively. Positive monoclonal strains were selected using chloramphenicol (40 μM) and validated by WB assay, designated as TgUAE1^{WT}c and TgUAE1^{C634S}c.

Mass spectrometry for RH TgUAE1-3HA strain identification

Freshly released tachyzoites (1×10^9) were filtered through 3 μm filters and centrifuged at 1000 × *g* for 10 min. The collected parasites were washed with PBS and lysed in a lysis buffer containing 150 mM NaCl, 1% Triton, 0.1% SDS, 0.5 mM EDTA, and 50 mM Tris-HCl (pH 7.5), supplemented with a complete Mini protease inhibitor tablet (Roche, Cat#11873580001), by incubating for 1 h at 4 °C. Following centrifugation at 21,000 × *g* for 15 min at 4 °C, the total protein extract was incubated with protein IgG beads for 4 h and then with α-HA magnetic beads (Thermo Fisher Scientific, Cat#88836) overnight at 4 °C. The protein complex bound to the magnetic beads was washed three times with wash buffer (50 mM Tris-HCl pH 7.5, 150 mM NaCl, 0.5 mM EDTA, protease inhibitor tablet). LDS Sample Buffer was added to the magnetic beads and heated at 95 °C for 6 min. The resulting sample was loaded onto an SDS-PAGE gel for electrophoresis. The adhesive strip containing the separated proteins was excised for mass spectrometry identification.

Cloning and purification of recombinant TgUAE1 protein

The coding sequence of TgUAE1 was amplified from the parasite cDNA using primers U5-F/R and inserted into the linearized pGEX-6P-1 vector for the fusion of TgUAE1 to the C terminus of GST. The plasmid was transformed into *E. coli* BL21 competent cells and protein expression was induced by Isopropyl β-D-1-Thiogalactopyranoside (IPTG) at 37 °C for 4 h. The recombinant GST-TgUAE1 proteins were purified using Glutathione SepharoseTM^{4B} (GE Healthcare) and verified by Coomassie blue staining and WB assay with an anti-GST antibody (dilution 1:2000, CMCTAG, Cat#AT0027).

Identification of TgUAE1 E1 activity in vitro

The activation and trans-thioesterification assays were performed on ice in reaction buffer (50 mM HEPES pH 7.5, 150 mM NaCl, and 5 mM $MgCl_2$). A mixture of 30 nM Flag-Ub (Sigma-Aldrich, Cat#U5507), 0.2 μM E1 (TgUAE1), and 100 μM ATP (Sigma-Aldrich, Cat#S1985) was incubated in the reaction buffer at room temperature for 5 min. Subsequently, an additional incubation of 5 min with 10 μM E2 (human CDC34, YouBi biotechnology, Cat#UBE-013) was carried out to initiate the trans-thioesterification of Ub. Two samples were prepared at each step, with one sample treated with 10 mM DTT and subjected to SDS-PAGE and WB. The Flag-Ub-containing bands were visualized using an Anti-Flag antibody. For the TAK-243 inhibition assay, a two-fold serial dilution of TAK-243 (GlpBio, GC32737) was performed with 30 nM Flag-Ub and 0.2 μM E1 (TgUAE1) in reaction buffer containing 2% DMSO. The dilutions ranged from 40 μM to 2.5 μM TAK-243. After adding 100 μM ATP, the mixture was incubated at room temperature for 30 min, followed by SDS-PAGE and WB.

Thermal stabilization experiment

Thermal stabilization experiments were conducted to verify the in vivo E1 activity of TgUAE1. Approximately 4×10^8 freshly egressed parasites were obtained by passage through a 3 μM filter followed by centrifugation. The parasites were resuspended in 1 ml of reaction solution containing 115 mM NaCl, 3 mM KCl, 2 mM $CaCl_2$, 1 mM $MgCl_2$, 3 mM NaH_2PO_4,10 mM HEPES, and 10 mM glucose. This suspension was prepared with or without adding 5 μM TAK-243 and incubated for 6 h at 37 °C. The sample was aliquoted into 100 μl per tube and subjected to thermal cycling on a PCR instrument at 10 different temperatures (37, 41, 43, 47, 50, 53, 56, 59, 63, and 67 °C) for 3 min. Subsequently, 12 μl of 10× lysis buffer was added to each tube, mixed thoroughly, and incubated on ice for 10 min. The lysates underwent three freeze-thaw cycles, involving freezing in liquid nitrogen and thawing at 37 °C. Following this, centrifugation was performed at 14,000 × *g* for 15 min. Western blot analysis used an anti-HA antibody to monitor changes in TgUAE1 protein levels under varying temperatures, with TgSAG1 protein as a negative control.

RT-qPCR

Total RNA was extracted from parasites using the Trizol reagent (Thermo Fisher Scientific, Cat#15596026) and converted into cDNA using HiScript II Reverse Transcriptase (Vazyme, R223-01). One microliter of cDNA was used as a template per qRT-PCR reaction, with specific primers targeting *Tgae1* (U6-F/R), Tgβ-Tubulin (U7-F/R), or *T. gondii* ER stress-related genes (*Tgpuf*, *Tgalg14*, *Tgtpp*, *Tgderlin1*, *Tgcrt*, *Tgsag2c*, U8/9/10/11/12/13-F/R). The reaction conditions followed the instructions of the ChamQ™ Universal SYBR® qPCR Master Mix (Vazyme, R711-02). The threshold cycle ($2^{-\Delta\Delta CT}$) method was used to evaluate the fold changes in transcripts, with Tgβ-Tubulin serving as the internal transcript control.

Western blot

The collected parasites were lysed on ice using a lysis buffer (50 mM Tris-HCl pH 7.5, 1% Triton, 0.1% SDS, 0.5 mM EDTA, 150 mM NaCl). Proteins were separated using 10% or 12% acrylamide gels and analyzed by WB using specific antibodies, including mouse anti-HA (Thermo Fisher Scientific, Cat#26183) at 1/2000, rabbit anti-Flag (Proteintech, Cat#20543-1-AP) at 1/2000, rabbit anti-Ub (Abcam, Cat#Ab7780) at 1/2000, rabbit anti-Ub-K48 (Abcam, ab140601) at 1/1000, rabbit anti-Ub-K63 (Abcam, ab179434) at 1/1000, mouse anti-Myc (Thermo Fisher, MA1-980) at 1/1000, and mouse anti-TgSAG1 (Abcam, Cat#Ab8313) at 1/5000.

Evaluation of mitochondrial integrity

To evaluate the influence of TgUAE1 depletion or TgUAE1 Cys634 mutation on mitochondrial integrity, each line was transiently transfected with the pMito-RFP plasmid, containing the mitochondrial matrix-targeting leader sequence of TgHsp60 fused with a red fluorescent protein (RFP)[61], before ATc treatment. IFA then observed mitochondrial morphology.

Immunofluorescence assay (IFA)

The IFA was carried out as previously described in ref. 62. Primary antibodies included mouse anti-HA at 1/800, anti-F1-β-ATPase (laboratory-prepared), mouse anti-TgCpn60 (laboratory-prepared) at 1/200, rabbit anti-ROP1[63] at 1/500, mouse anti-MIC3 antibody[64] at 1/500, mouse anti-TgSAG1 antibody(Abcam, Cat# ab8313) at 1/5000, rabbit anti-TgTubulin antibody at 1/1000. Secondary antibodies used were goat anti-mouse or goat anti-rabbit Alexa Fluor 488 (YEASEN, Shanghai, Cat# 33106ES60), goat anti-rabbit Alexa Fluor 594 (YEASEN, Shanghai, Cat# 33112ES60), and goat anti-rabbit Alexa Fluor 647 (YEASEN, Shanghai, Cat# 33113ES60).

Plaque assay

Standard plaque assays were conducted with or without ATc treatment for 7 days, following established protocols[29]. The plates were scanned, and plaque areas were quantified using ImageJ software.

Invasion assay

Intracellular parasites were incubated with or without 0.5 μg/ml ATc for 72 h, then mechanically released using a 27-gauge needle and purified from host cell debris via a 3 μm filter. These purified parasites were added to a monolayer of HFFs in a 24-well plate, incubated on ice for 30 min, and then incubated at 37 °C for an additional 1 h. The invasion was halted by fixation with 4% (w/v) paraformaldehyde, and invasion rates were determined by IFA. Extracellular parasites were labeled with a mouse anti-TgSAG1 antibody[65] prior to permeabilization, while intracellular parasites were labeled with a rabbit anti-GAP45 antibody post-permeabilization. The assays were performed in triplicate, and at least 100 tachyzoites were counted per experiment.

Intracellular proliferation assay

Monolayers of HFFs were infected with freshly egressed tachyzoites, pre-treated with 0.5 μg/ml ATc for 72 h or left untreated, in 24-well plates at a multiplicity of infection (MOI) of 4. After 24 h, the slides were washed with PBS and fixed with 4% (w/v) paraformaldehyde for 30 min, followed by staining with a mouse anti-TgSAG1 antibody. The number of parasites within at least 100 vacuoles was counted, and the experiment was repeated three times.

Egress assay

HFF monolayers on glass coverslips in 24-well plates were infected with 8×10^4 purified tachyzoites, pre-treated with or without 0.5 μg/ml ATc. After 24 h of incubation, the plates were washed with 1 ml/well DPBS, treated with HBSS containing 1 μM calcium ionophore and incubated for 2.5 min at 37 °C in 5% CO2. The samples were then fixed with a solution containing 4% (w/v) paraformaldehyde. After permeabilization, a mouse anti-TgGRA3 antibody was used to label the vacuoles and the rabbit anti-TgGAP45 antibody was used to label the parasites. The percentage of ruptured vacuoles among approximately 100 vacuoles was counted. The experiment was repeated three times.

Gliding assay

For the gliding assay, coverslips were coated with 1 mg/ml poly-L-lysine for 2 h at room temperature. Freshly released tachyzoites were collected by centrifugation and resuspended in 200 μl of Ringer buffer (155 mM NaCl, 3 mM KCl, 1 mM $CaCl_2$, 1 mM $MgCl_2$, 3 mM NaH_2PO_4, 10 mM HEPES, 10 mM glucose), then deposited onto coverslips for incubation at 37 °C for 10 min. Parasites were fixed with a solution containing 4% (w/v) paraformaldehyde and 0.05% glutaraldehyde, followed by IFA using a mouse anti-TgSAG1 antibody to visualize the gliding trails.

In vitro evaluation of the anti-toxoplasma activity and cytotoxicity of TAK-243

HFFs were digested and seeded at 500 cells/well in the central 60 wells of a 96-well plate (85 μl per well) and cultured for 24 h. TAK-243 stock solution (10 mM) was serially diluted to generate an initial working concentration of 1 μM. A 9-point concentration gradient (200 nM to 0.39 nM) was prepared via sequential two-fold dilution in culture medium (final volume 170 μl/well), with the 10th well serving as a drug-free control. The RH-2F strain of *T. gondii* tachyzoites was filtered twice, centrifuged (1000 × *g*, 10 min), and resuspended in culture medium to 10 parasites/μl. Each well received 10 μl parasite suspension (final 1 parasite/μl). After 72 h incubation, parasite egress in control wells was confirmed. Chlorophenol red-β-D-galactopyranoside (CPRG, 20 μl/well) was added, followed by 24 h incubation. β-galactosidase activity reflecting parasite viability was quantified at 630 nm for EC_{50} determination. Uninfected wells were treated with 20 μl CellTiter 96® AQueous One Solution Reagent after 72 h drug exposure. Following 3 h incubation, cellular metabolic activity was measured at 490 nm to evaluate TAK-243-induced proliferation inhibition.

Transcriptomic analysis

Four replicates of cKD-TgUAE1 transgenic parasites cultured with 0.5 μg/ml ATc (knockdown line) and DMSO (parental strain) were prepared and sent to Lian Chuan BioTech Co. (Hangzhou, China) for TgUAE1-specific transcriptome construction and analysis. Total RNA was extracted from each culture, and mRNA was isolated from the total RNA, fragmented, and used to synthesize first- and second-strand cDNAs. The double-stranded cDNA was purified and end-repaired, and an adenine was added. The final cDNA library was sequenced on an Illumina NovaSeq TM 6000 platform.

Clean tags generated by filtering raw reads from the sequencing were mapped to the *T. gondii* genome (ToxoDB; http://toxodb.org). Data were normalized as fragments per kilobase of exon per million fragments mapped (FPKM). DEGs were identified with $\log_2 R$ of ≤ −1 (downregulated) or ≥1 (upregulated) and $q < 0.05$. These DEGs were annotated using known or putative gene information from the NCBI protein databases and subjected to Gene Ontology (GO) analysis (http://www.geneontology.org/) for GO term enrichment in three functional classes ($p < 0.05$) and KEGG analysis (http://www.kegg.jp/kegg) for pathway enrichment ($p < 0.05$).

Ubiquitination quantitative proteomics analysis

Two replicates of TATi1 Δ*Ku80* and cKD-TgUAE1 transgenic parasites cultured with 0.5 μg/ml ATc were prepared and sent to PTM BioLab Co. (Hangzhou, China) for TgUAE1-specific ubiquitination quantitative proteomics analysis. Total protein was extracted from each culture, digested with trypsin, and the peptides were dissolved in IP buffer solution for liquid chromatography-mass spectrometry analysis. The secondary mass spectrometry data were analyzed using Maxquant (v1.6.15.0) and searched against the Toxoplasma_gondii_5811_ToxoDB-60_TgondiiGT1_20221212.fasta database, containing 8460 sequences. Reverse libraries were used to calculate the false positive rate from random matches, and standard contaminant libraries were included to eliminate contaminating proteins. Based on database search results, quality control analysis was conducted at both peptide and protein levels. Quantitative analysis of proteins was performed, assessing their distribution and reproducibility, and displaying the distribution of sample quantitative intensity values. To screen for differences between two groups based on quantitative results, we first selected the samples for comparison. The mean relative quantification value of each protein across the two replicates in the comparison groups was used to calculate the fold change (FC). For instance, to calculate the fold change between sample groups A and B for a given protein, the following formula was applied, where R represents the relative quantification value of the protein, i denotes the sample, and k refers to the protein: $FC_{A/B,k}=Mean((R_{ik,i}\in A)/(R_{ik,i}\in B))$. To determine the significance of the differences, the standard coefficient of variation (CV) for each protein in

the two comparison groups was calculated as an indicator of significance, with a default threshold of $CV < 0.1$. The formula used was: $CV_k = SD(A_{1k}/B_{1k}, A_{2k}/B_{2k})/Mean(A_{1k}/B_{1k}, A_{2k}/B_{2k})$. Common functional annotations of identified proteins were performed using GO, KEGG, Protein domain, COG/KOG, and STRING databases.

Statistics and reproducibility

GraphPad Prism 9 software was used to analyze the experimental data. Each experiment was independently repeated at least three times. For normally distributed data, Student's *t*-test was used for comparisons between two groups, and one-way ANOVA was used for comparisons between three or more groups. For non-normally distributed data, the Kruskal-Wallis test with Dunn's multiple comparisons was applied. Results are presented as the mean ± standard deviation (SD), with $P < 0.05$ considered statistically significant.

Reporting summary

Further information on research design is available in the Nature Portfolio Reporting Summary linked to this article.

Data availability

All data generated or analyzed during this study are included in the manuscript and its associated supplemental files. The numerical source data underlying the graphs in our study can be found in the Supplementary Data 5. The uncropped and unedited blot/gel images have been included as Supplementary Fig.(s) in the Supplementary Information file. The RNA sequencing (RNA-seq) data from this study are available at the NCBI Gene Expression Omnibus under accession number GSE240648. The mass spectrometry ubiquitination quantitative proteomics data have been deposited in the ProteomeXchange Consortium via the PRIDE[66] partner repository with the dataset identifier PXD045018.

Received: 2 September 2024; Accepted: 30 April 2025;
Published online: 10 May 2025

References

1. Dubey, J. P. *Toxoplasmosis of Animals and Humans*. (Toxoplasmosis of Animals and Humans, 2016).
2. Gao, J. M. et al. Genetic analyses of Chinese isolates of *Toxoplasma gondii* reveal a new genotype with high virulence to murine hosts. *Vet. Parasitol.* **241**, 52–60 (2017).
3. Dubey, J. P. Toxoplasmosis in pigs-The last 20 years. *Vet. Parasitol.* **164**, 89–103 (2009).
4. Neville, A. J. et al. Clinically available medicines demonstrating anti-*Toxoplasma* activity. *Antimicrob. Agents Ch* **59**, 7161–7169 (2015).
5. Ben-Harari, R. R., Goodwin, E. & Casoy, J. Adverse event profile of pyrimethamine-based therapy in Toxoplasmosis: A Systematic Review. *Drugs RD* **17**, 523–544 (2017).
6. Montazeri, M. et al. Drug Resistance in *Toxoplasma gondii*. *Front. Microbiol.* **9**, https://doi.org/10.3389/fmicb.2018.02587 (2018).
7. Shaw, M. K., He, C. Y., Roos, D. S. & Tilney, L. G. Proteasome Inhibitors block intracellular growth and replication of *Toxoplasma gondii*. *Parasitology* **121**, 35–47 (2000).
8. Popovic, D., Vucic, D. & Dikic, I. Ubiquitination in disease pathogenesis and treatment. *Nat. Med.* **20**, 1242–1253 (2014).
9. Pohl, C. & Dikic, I. Cellular quality control by the ubiquitin-proteasome system and autophagy. *Science* **366**, 818–822 (2019).
10. Chowdhury, M., Enenkel, C., Ramos, P. C., Coffino, P. & Wendler, P. Intracellular Dynamics of the Ubiquitin-Proteasome-System. *other* (2015).
11. Callis, J. The ubiquitination machinery of the ubiquitin system. *Arabidopsis Book* **12**, e0174 (2014).
12. Wang, X. L. et al. Ubiquitination of serine, threonine, or lysine residues on the cytoplasmic tail can induce ERAD of MHC-I by viral E3 ligase mK3. *J. Cell Biol.* **177**, 613–624 (2007).
13. Jin, J. P., Li, X., Gygi, S. P. & Harper, J. W. Dual E1 activation systems for ubiquitin differentially regulate E2 enzyme charging. *Nature* **447**, 1135–U1117 (2007).
14. Lee, I. & Schindelin, H. Structural insights into E1-catalyzed ubiquitin activation and transfer to conjugating enzymes. *Cell* **134**, 268–278 (2008).
15. Agrawal, S. et al. An apicoplast localized ubiquitylation system is required for the import of nuclear-encoded plastid proteins. *Plos Pathog.* **9**, e1003426 (2013).
16. Xiao, Q. Q. et al. Uba1: a potential ubiquitin-like activator protein of urm1 in *Toxoplasma gondii*. *International J. Mol. Sci.***23**, https://doi.org/10.3390/ijm (2022).
17. Green, J. L., Wu, Y., Encheva, V., Lasonder, E. & Holder, A. A. Ubiquitin activation is essential for schizont maturation in *Plasmodium falciparum* blood-stage development. *PLoS Pathog.* **16**, e1008640 (2020).
18. Barghout, S. H. & Schimmer, A. D. E1 enzymes as therapeutic targets in cancer. *Pharm. Rev.* **73**, 1–58 (2021).
19. Chen, J. J. et al. Mechanistic studies of substrate-assisted inhibition of ubiquitin-activating enzyme by adenosine sulfamate analogues. *J. Biol. Chem.* **286**, 40867–40877 (2011).
20. Herneisen, A. L. et al. Identifying the target of an antiparasitic compound in toxoplasma using thermal proteome profiling. *ACS Chem. Biol.* **15**, 1801–1807 (2020).
21. Corpas-Lopez, V. et al. Pharmacological validation of n-myristoyltransferase as a drug target in *leishmania donovani*. *ACS Infect. Dis.* **5**, 111–122 (2019).
22. Dziekan, J. M. et al. Identifying purine nucleoside phosphorylase as the target of quinine using cellular thermal shift assay. *Sci. Transl. Med.* **11**, https://doi.org/10.1126/scitranslmed.aau3174 (2019).
23. Hua, Q. Q. et al. Two small-molecule inhibitors of *Toxoplasma gondii* proliferation in vitro. *Front. Cell Infect. Mi* **13**, https://doi.org/10.3389/fcimb.2023.1145824 (2023).
24. Seeber, F. & Boothroyd, J. C. *Escherichia coli* β-galactosidase as an in vitro and in vivo reporter enzyme and stable transfection marker in the intracellular protozoan parasite *Toxoplasma gondii*. *Gene* **169**, 39–45 (1996).
25. Sidik, S. M. et al. A genome-wide crispr screen in toxoplasma identifies essential apicomplexan genes. *Cell* **166**, 1423–1425 (2016).
26. Zhuang, J. L. et al. Ubiquitin-activating enzyme inhibition induces an unfolded protein response and overcomes drug resistance in myeloma. *Blood* **133**, 1572–1584 (2019).
27. Hyer, M. L. et al. A small-molecule inhibitor of the ubiquitin activating enzyme for cancer treatment. *Nat. Med.* **24**, 186–193 (2018).
28. Joyce, B. R., Tampaki, Z., Kim, K., Wek, R. C. & Sullivan, W. J. The unfolded protein response in the protozoan parasite *Toxoplasma gondii* features translational and transcriptional control. *Eukaryot. Cell* **12**, 979–989 (2013).
29. Wu, M. M. et al. *Toxoplasma gondii* autophagy-related protein ATG7 maintains apicoplast inheritance by stabilizing and lipidating ATG8. *Bba-Mol Basis Dis.* **1870**, https://doi.org/10.1016/j.bbadis.2023.166891 (2024).
30. Paugam, A., Creuzet, C., Dupouy-Camet, J. & Roisin, M. P. Evidence for the existence of a proteasome in *Toxoplasma gondii*: intracellular localization and specific peptidase activities. *Parasite* **8**, 267–273 (2001).
31. Fellows, J. D., Cipriano, M. J., Agrawal, S., Striepen, B. & Weiss, L. M. A plastid protein that evolved from ubiquitin and is required for apicoplast protein import in *Toxoplasma gondii*. *mBio* **8**, e00950–17 (2017).
32. Sheikh, M. O. et al. O(2) sensing-associated glycosylation exposes the F-box-combining site of the Dictyostelium Skp1 subunit in E3 ubiquitin ligases. *J. Biol. Chem.* **292**, 18897–18915 (2017).
33. Silmon de Monerri, N. C. et al. The Ubiquitin Proteome of *Toxoplasma gondii* Reveals Roles for Protein Ubiquitination in Cell-Cycle Transitions. *Cell Host Microbe* **18**, 621–633 (2015).

34. Naumov, A. et al. The Toxoplasma Centrocone Houses Cell Cycle Regulatory Factors. *mBio* **8**, https://doi.org/10.1128/mBio.00579-17 (2017).
35. Mehta, S. & Sibley, L. D. *Toxoplasma gondii* actin depolymerizing factor acts primarily to sequester G-actin. *J. Biol. Chem.* **285**, 6835–6847 (2010).
36. Mehta, S. & Sibley, L. D. Actin depolymerizing factor controls actin turnover and gliding motility in *Toxoplasma gondii*. *Mol. Biol. Cell* **22**, 1290–1299 (2011).
37. Gonzalez, V. et al. Host cell entry by apicomplexa parasites requires actin polymerization in the host cell. *Cell Host Microbe* **5**, 259–272 (2009).
38. Bichet, M. et al. Genetic impairment of parasite myosin motors uncovers the contribution of host cell membrane dynamics to Toxoplasma invasion forces. *BMC Biol.* **14**, 97 (2016).
39. Dubremetz, J. F. Rhoptries are major players in *Toxoplasma gondii* invasion and host cell interaction. *Cell Microbiol.* **9**, 841–848 (2007).
40. Dubois, D. J. et al. *Toxoplasma gondii* HOOK-FTS-HIP complex is critical for secretory organelle discharge during motility, invasion, and egress. *mBio* **14**, e0045823 (2023).
41. Ryning, F. W. & Remington, J. S. Effect of cytochalasin D on *Toxoplasma gondii* cell entry. *Infect. Immun.* **20**, 739–743 (1978).
42. Andenmatten, N. et al. Conditional genome engineering in *Toxoplasma gondii* uncovers alternative invasion mechanisms. *Nat. Methods* **10**, 125–127 (2013).
43. Roos-Mattjus, P. & Sistonen, L. The ubiquitin-proteasome pathway. *Ann. Med.* **36**, 285–295 (2004).
44. Finger, A., Knop, M. & Wolf, D. H. Analysis of two mutated vacuolar proteins reveals a degradation pathway in the endoplasmic reticulum or a related compartment of yeast. *Eur. J. Biochem* **218**, 565–574 (1993).
45. Senft, D. & Ronai, Z. A. UPR, autophagy, and mitochondria crosstalk underlies the ER stress response. *Trends Biochem Sci.* **40**, 141–148 (2015).
46. Qu, J. Y., Zou, T. T. & Lin, Z. H. The roles of the ubiquitin-proteasome system in the endoplasmic reticulum stress pathway. *Int. J. Mol. Sci.* **22**, https://doi.org/10.3390/ijms22041526 (2021).
47. Hetz, C. & Papa, F. R. The Unfolded Protein Response and Cell Fate Control. *Mol. Cell* **69**, 169–181 (2018).
48. Costa-Mattioli, M. & Walter, P. The integrated stress response: From mechanism to disease. *Science* **368**, 384 (2020).
49. Brodsky, J. L. & Chiosis, G. Hsp70 molecular chaperones: Emerging roles in human disease and identification of small molecule modulators. *Curr. Top. Med. Chem.* **6**, 1215–1225 (2006).
50. Mitra, P., Deshmukh, A. S. & Choudhury, C. Molecular chaperone function of stress inducible Hsp70 is critical for intracellular multiplication of *Toxoplasma gondii*. *Bba-Mol, Cell Re.s* **1868**, https://doi.org/10.1016/j.bbamcr.2020.118898 (2021).
51. Whatley, B. R., Li, L. & Chin, L. S. The ubiquitin-proteasome system in spongiform degenerative disorders. *Biochim Biophys. Acta* **1782**, 700–712 (2008).
52. Seidi, A. et al. Elucidating the mitochondrial proteome of *Toxoplasma gondii* reveals the presence of a divergent cytochrome c oxidase. *Elife* **7**, https://doi.org/10.7554/eLife.38131 (2018).
53. Lehmann, G. et al. Ubiquitination of specific mitochondrial matrix proteins. *Biochem Biophys. Res Commun.* **475**, 13–18 (2016).
54. Lemmer, I. L., Willemsen, N., Hilal, N. & Bartelt, A. A guide to understanding endoplasmic reticulum stress in metabolic disorders. *Mol Metab* **47**, https://doi.org/10.1016/j.molmet.2021.101169 (2021).
55. Sugi, T., Masatani, T., Murakoshi, F., Kawazu, S. & Kato, K. Microplate assay for screening *Toxoplasma gondii* bradyzoite differentiation with DUAL luciferase assay. *Anal. Biochem* **464**, 9–11 (2014).
56. Sheiner, L. et al. A systematic screen to discover and analyze apicoplast proteins identifies a conserved and essential protein import factor. *PLoS Pathog.* **7**, e1002392 (2011).
57. Kumar, S., Stecher, G. & Tamura, K. Mega7: molecular evolutionary genetics analysis version 7.0 for bigger datasets. *Mol. Biol. Evol.* **33**, 1870–1874 (2016).
58. Nicholas, K. & Nicholas, H. GeneDoc: a tool for editing and annotating multiple sequence alignments. (1997).
59. Wang, S., Li, W., Liu, S. & Xu, J. RaptorX-Property: a web server for protein structure property prediction. *Nucleic Acids Res* **44**, W430–W435 (2016).
60. Li, X. Z. et al. Induction of Autophagy interferes the tachyzoite to bradyzoite transformation of *Toxoplasma gondii*. *Parasitology* **143**, 639–645 (2016).
61. van Dooren, G. G. et al. A novel dynamin-related protein has been recruited for apicoplast fission in *Toxoplasma gondii*. *Curr. Biol.* **19**, 267–276 (2009).
62. Liu, S. X. et al. Characterization of the molecular mechanism of the autophagy-related Atg8-Atg3 protein interaction in *Toxoplasma gondii*. *J. Biol. Chem.* **293**, 14545–14556 (2018).
63. Lentini, G. et al. Characterization of Toxoplasma DegP, a rhoptry serine protease crucial for lethal infection in mice. *PLoS One* **12**, e0189556 (2017).
64. Qiu, J. et al. Identification of a TNF-alpha inducer MIC3 originating from the microneme of non-cystogenic, virulent *Toxoplasma gondii*. *Sci. Rep.* **6**, 39407 (2016).
65. Yang, Y. M. et al. The first apicoplast tRNA thiouridylase plays a vital role in the growth of *Toxoplasma gondii*. *Front. Cell Infect. Mi.* **12**, https://doi.org/10.3389/fcimb.2022.947039 (2022).
66. Perez-Riverol, Y. et al. The PRIDE database resources in 2022: a hub for mass spectrometry-based proteomics evidences. *Nucleic Acids Res.***50**, D543–D552 (2022).

Acknowledgements

We extend our gratitude to Dr. Sébastien Besteiro (Université de Montpellier, France) for providing the TATi1 Δ*Ku80* and RH-2F strains, as well as the anti-ROP1 and anti-MIC3 antibodies. We also thank Dr. William J. Sullivan, Jr. (Indiana University School of Medicine, IN) for supplying the RH Δ*Ku80* strain and the pLIC-3HA-DHFR-Ts vector, Dr. Bang Shen (Huazhong Agricultural University, China) for the pSAG1::Cas9-U6::sgUPRT vector, Dr. Aifang Du (Zhejiang University, China) for the anti-GAP45 antibody, and Dr. Giel G van Dooren (Australian National University, Australia) for the pMito-RFP plasmid. Grateful to all members of the Tan laboratory for their insightful comments. Special thanks to the Scientific Research Center of Wenzhou Medical University for providing consultation and access to instruments that supported this work. This work was supported in part by grants from the National Natural Science Foundation of China (82402659), the Natural Science Foundation of Zhejiang Province (LQN25H190007), the Talent Project of Wenzhou Medical University (89222021) to Y-N.M.; the National Natural Science Foundation of China (81971962, 82172303, 82372282), the Key Project of Natural Science Foundation of Zhejiang Province (LZ22H190001) to F T; and the Ministry of Education Industry-University Cooperative Education Program (231004408283815) to F-J.L. All funders had no role in the design of the study and collection, analysis, and interpretation of data as well as in writing the manuscript.

Author contributions

Q-X.Z. and D-Q.L. generated all transgenic lines and drafted the original manuscript. Q-X.Z., D-Q.L., S-Y. T., Y. L., M-W.C., X. T. and Y-T.W. conducted experiments, validated methodologies, and analyzed data. F-J.L., F.T. and Y-N.M. conceived the study approach, supervised the project, and revised the manuscript. All authors read and approved the final manuscript.

Competing interests

The authors declared no competing interests.

Additional information

Supplementary information The online version contains supplementary material available at https://doi.org/10.1038/s42003-025-08149-x.

Correspondence and requests for materials should be addressed to Feng Tan or Ya-ni Mou.

Peer review information *Communications Biology* thanks Budhaditya Mukherjee, Masahiro Yamamoto and the other, anonymous, reviewer(s) for their contribution to the peer review of this work. Primary Handling Editors: Nishith Gupta and Johannes Stortz.